UNIVERSITA' DEGLI STUDI DI MESSINA

Dipartimento di Medicina Clinica e Sperimentale

Dottorato di Ricerca in Scienze Biomediche Cliniche e Sperimentali

XXXII ciclo

Coordinatore: Ch.mo Prof. Francesco Squadrito

Role of noninvasive imaging in the management of skin cancer

Tesi di Dottorato di
Dott.ssa Roberta Giuffrida

Tutor/relatore
Chiar.ma Prof.ssa Serafinella P. Cannavò

Correlatore
Chiar.ma Prof.ssa Iris Zalaudek

Anno Accademico: 2018-2019

Agli affetti e ai luoghi del cuore, vicini e lontani.

The present PhD thesis is the result of my research activity conducted at the "Non Melanoma Skin Cancer Unit", Division of Dermatology, Medical University of Graz (Austria), under the supervision of Prof. I. Zalaudek, and Department of Clinical and Experimental Medicine, Section of Dermatology, University of Messina (Italy), under the supervision of Prof. S.P. Cannavò and Dott. F. Borgia.

INDEX

CHAPTER 1

1.1 INTRODUCTION

Over the years, the use of imaging technology has changed the way in which the physicians take care of their patients. In the past decades, many noninvasive imaging techniques have been involved in detecting, diagnosing, and even treating several dermatologic disorders. In particular, they have been increasingly used for diagnosis and management of skin cancers, revealing more accuracy and precision than unaided visual inspection.[1]

The most used types of imaging for the detection and monitoring of atypical skin lesions and for the early recognition of melanoma and non-melanoma skin cancer are total body photography (TBP) and dermoscopy. However, many other types of cutaneous imaging approaches have been developed and are currently used in specialized centres. They include ultrasound sonography, reflectance confocal microscopy, optical coherence tomography, electrical impedance techniques, Raman spectroscopy, multispectral imaging, fluorescence imaging and multispectral optoacoustic tomography.[2,3]

Digital photography is widely used in Dermatology both for clinical practice and research. It is useful to follow clinical evolution of a disease, document changes before and after treatment, identify suspicious skin lesions and predict

skin cancer.[4] Images may be printed, filed in a digital medical record or, linked with medical information, transmitted rapidly via smartphone or personal computer to a dermatologist for remote evaluation (*Teledermatology*), especially in places where it is difficult to access to healthcare services.[5,6]

Total body photography is a type of digital photography widely used by dermatologists, consisting of the capture of a series of sectional photos of the whole body's skin surface, with the aim to track any potential changes over the time.[2] Digital images can be stored electronically and used for comparisons at follow-up, or analysed by specific software for computer-assisted diagnosis of skin cancer.[4]

Dermoscopy or ***dermatoscopy*** or ***epiluminescence microscopy*** is a rapid and inexpensive noninvasive tool allowing a magnified (approximately 10x) *in vivo* and *en face* visualization of the skin surface, with the observation of morphologic structures that are located in the epidermis and papillary dermis, correlated with specific histopathologic features.[7,10] It has been shown to have a sensitivity and specificity in the detection of melanoma significantly higher than the naked-eye examination.[1,8,9]

Videodermoscopy requires a videocamera fitted to a headpiece equipped with lenses providing a magnification ranging from 10x to 1000x and allowing visualization of the images on a monitor, with the possibility to store them on a personal computer.

Sequential digital dermoscopic imaging (SDDI) is a monitoring technique that allows storage and retrieval of dermoscopic pictures of melanocytic and non-melanocytic lesions and their comparison at different time intervals, in order to detect any suspicious change.[11] It mainly increases specificity for skin cancer detection while simultaneously decreasing the number of unnecessary biopsies of biologically benign lesions.[12,13]

A large meta-analysis reported that, by using SDDI, 54.6% of melanomas can be excised in situ.[14,15]

The effectiveness of dermoscopy has been also well described for the diagnosis of keratinocyte skin cancers (actinic keratosis, basal cell carcinoma, Bowen's disease and invasive squamous cell carcinoma)[16,17] (Figure 1.1), as well as for their presurgical assessment or evaluation of response to topical treatment and long-term follow-up.[9,18-20]

Finally, the combination of TBP and dermoscopy results more accurate than the two strategies separately, especially in the detection of melanomas in early stages.[21-24]

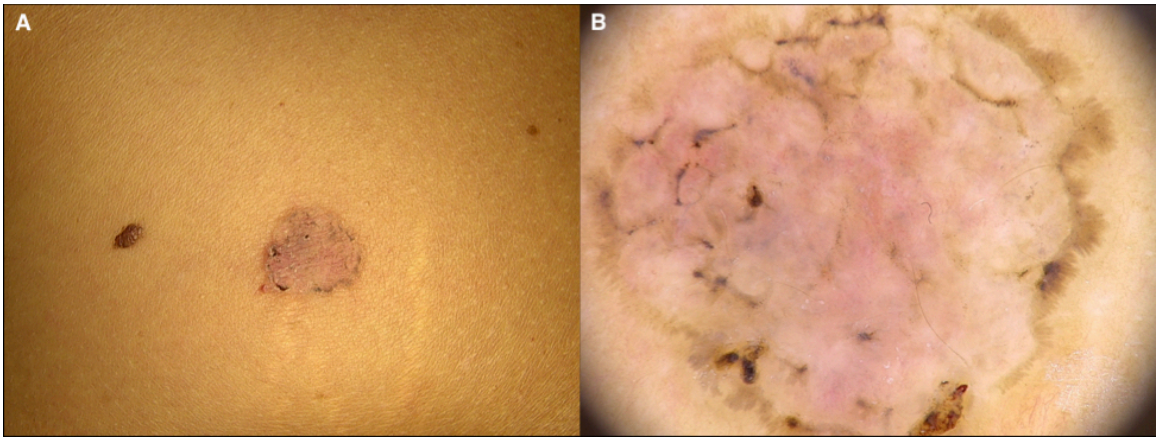

Figure 1.1. A) A round pink patch with a pigmented edge, located on the trunk of a 39-year-old woman, histopathologically revealing a superficial basal cell carcinoma. B) Dermoscopy showing multiple brown dots, short fine superficial telangiectasias, spoke-wheel-like structures and leaf-like areas.

Reflectance confocal microscopy is a noninvasive optical technology that enables real-time *in vivo* or *ex vivo* imaging of skin lesions at nearly histologic resolution (0.5-1 μm). It uses a focused laser beam to illuminate a specific point within the skin and measures the reflection of light from that point, providing serial horizontal black and white images of the layers of the epidermis and the upper dermis, related to the contrast from different refractive indexes of tissues and cell structures (refractive structures appear bright, while non-refractive tissues appear dark).[25-30]

Over the years, a lot of interest has been shown in using this technique in the diagnosis and monitoring of treatment of skin cancers, especially large lesions on cosmetically sensitive areas (Figure 1.2). [27-32]

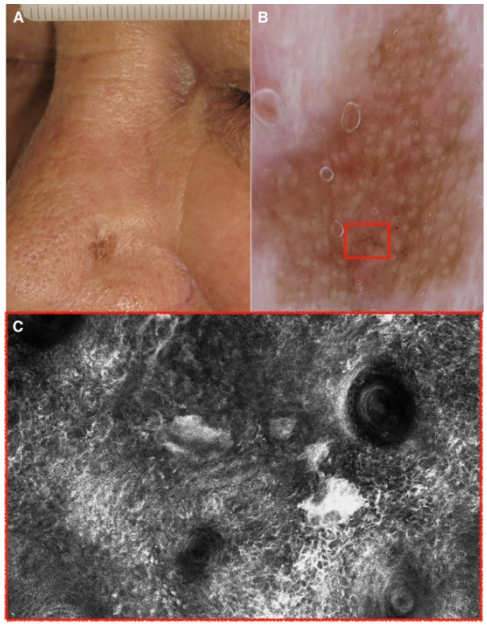

Figure 1.2. A) Clinical picture of a 68-year-old man with a lentigo maligna of the nose. B) Dermoscopy shows a brown pseudo-network with brown globules (red box). C) Corresponding reflectance confocal microscopy highlights atypical cells surrounding hair follicles and junctional melanocytes nests.

RCM features of melanocytic and non-melanocytic lesions are well established, showing a high sensitivity and specificity for their diagnosis.[33-37] RCM is a powerful tool, but it has some practical disadvantages, such as high cost and time required for evaluation of large or multiple lesions, as well as training and experience of the physician.

High-frequency ultrasonography (HF-US) is a fast noninvasive diagnostic medical tool that uses sound waves with frequency higher than 7 MHz, allowing visualization of the skin and subcutaneous tissue. It can be performed alone or in combination with Doppler ultrasound, in order to study vascular morphology and blood flow in real time.[3,38,39] In the field of dermato-oncology, it has been employed to perform an initial differential

skin cancer diagnosis, measure tumor depth, delineate preoperative surgical margins, assess loco-regional tumor spread, detect tumor recurrence and evaluate efficacy of therapy.[3]

All cutaneous malignancies appear as hypoechoic areas, often with prominent vascularity, in ultrasound images.[3]

Optical coherence tomography (OCT) is a noninvasive diagnostic technology allowing a real-time, *in vivo*, cross-sectional imaging of skin morphology.[29] It works similarly to ultrasound, but employs light with long wavelength instead of sound waves.[29] Dynamic OCT enables the *in vivo* evaluation of superficial blood vessels and their distribution within specific lesions.[33]

Compared with RCM, it allows imaging at a greater penetration depth, with a significantly lower cellular resolution.[40]

OCT has been shown to be a useful diagnostic tool for the early detection of skin cancer (Figure 1.3).[41-43]

Limitations of OCT include high costs and the need for specialized training for image interpretation.[43]

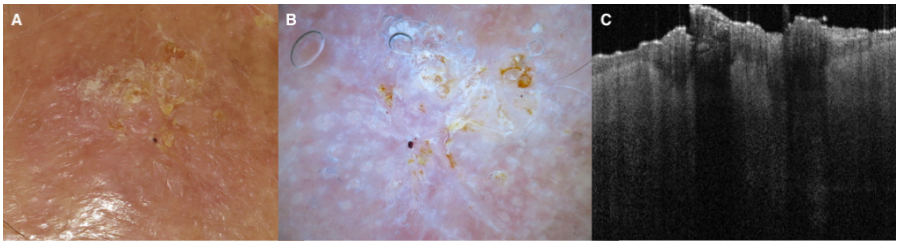

Figure 1.3. A) Slightly raised hyperkeratotic lesion located on the scalp in a 96-year old man. Histopathology revealed an invasive well differentiated squamous cell carcinoma. B) Dermoscopic image showing a predominant central keratin mass. C) Optical coherence tomography showing bright surface, focal hyperkeratosis, acanthosis and interruption of the dermo-epidermal junction.

The technology of ***electrical impedance*** measurements in the detection of skin cancer has become a topic of great interest among dermatologists in the last decades. It is based on the principle that malignant transformation of the cells alters their physiological electrical impedance (resistance to an injected electrical stimulus).[44,45]

Electrical impedance spectroscopy (EIS) is a type of safe, rapid, noninvasive and cost-effective technique first employed for the detection of melanoma, showing high sensitivity but low specificity.[45,46]

EIS device consist of a handheld probe with a disposable electrode necessary to apply an electrical current to the skin, receiving back the resulting current from the tissue.[45,46]

The new generation of EIS devices permits integration of dermoscopy images of skin lesions in the patient's file.[47] This method does not discern between different skin cancers, but helps physicians to differentiate between

benign and malignant lesions, both melanocytic and non-melanocytic.[47] In recent years, *electrical impedance tomography* (EIT), which uses low-frequency electrical current for imaging the differences in impedance between tissues, has been evaluated with the aim to exceed the limits of EIS lesions (small lesions or measurements on hyper-vascularized body areas).[47,48]

Raman spectroscopy is a spectroscopic vibrational molecular technique capable of measuring the inelastic monochromatic scattering of light by matter.[49] Raman spectra of human skin is obtained by laser excitation, using a near infrared light source (785-nm diode laser). The procedure has been evaluated in skin cancer diagnosis, showing high sensitivity but low specificity in differentiating between benign and malignant lesions (melanocytic and non-melanocytic).[50]

Other noninvasive optical techniques have arisen in the last few decades as tools for skin cancer detection and screening, and many other are in development. Among them, ***multispectral imaging*** was employed for the evaluation of pigmented skin lesions; it uses a light of different wavelengths penetrating the skin and gives sequences of images that are analysed by a computer algorithm for different features.[38] ***Fluorescence-based imaging*** is a well studied imaging strategy that has been used in detecting and mapping skin tumors, characteristically more fluorescent than healthy tissue.[3]

Multispectral optoacoustic tomography (MSOT) is a high-resolution noninvasive imaging tool based on the photoacoustic effect, merging optical illumination and ultrasound. It has been used in patients with melanoma and NMSC for tumor detection and presurgical margin assessment.[29,44]

Further novel noninvasive imaging methods, combined imaging modalities and artificial intelligence algorithms, are currently under investigation and in the near future will assist and improve the management of patients with skin cancers.

1.2. AIMS

In order to have more insights on the use of noninvasive imaging in the management of skin cancer, we aimed to:

a) evaluate clinical and dermoscopic criteria of nevus-associated melanoma;

b) assess the accuracy of dermoscopy compared to clinical examination in the detection of borders of basal cell carcinoma (BCC) and describe the most common dermoscopic findings in the clinically healthy tissue surrounding BCC, in case of not-matching clinically and dermoscopically detected margins;

c) evaluate the diagnostic accuracy of electrical impedance spectroscopy in the diagnosis of actinic keratosis (AK) and subclinical lesions in comparison to the naked eye examination and dermoscopy.

REFERENCES

1. Conforti C, Giuffrida R, Vezzoni R et al. Dermoscopy and the experienced clinicians. Int J Dermatol. 2019 Jun 20.
2. Psaty EL, Halpern AC. Current and emerging technologies in melanoma diagnosis: the state of the art. Clin Dermatol. 2009; 27: 35-45.
3. Schneider SL, Kohli I, Hamzavi IH et al. Emerging imaging technologies in dermatology: Part I: Basic principles. J Am Acad Dermatol. 2019; 80: 1114-20.
4. Dengel LT, Petroni GR, Judge J et al. Total body photography for skin cancer screening. Int J Dermatol. 2015; 54: 1250-4.
5. Tensen E, van der Heijden JP, Jaspers MW, Witkamp L. Two Decades of Teledermatology: Current Status and Integration in National Healthcare Systems. Curr Dermatol Rep. 2016; 5:96-104.
6. Walocko FM, Tejasvi T. Teledermatology Applications in skin cancer diagnosis. Dermatol Clin. 2017; 35: 559-63.
7. Conforti C, Giuffrida R, Retrosi C et al. Two controversies confronting dermoscopy or dermatoscopy: nomenclature and results. Clinics in Dermatology. 2019; 37: 597-9.
8. Vestergaard ME, Macaskill P, Holt PE, Menzies SW. Dermoscopy compared with naked eye examination for the diagnosis of primary

melanoma: a meta-analysis of studies performed in a clinical setting. Br J Dermatol. 2008; 159: 669-76.

9. Resende FS, Conforti C, Giuffrida R et al. Raised vulvar lesions: be aware! Dermatol Pract Concept. 2018 Apr 30;8(2):158-161.
10. Micali G, Lacarrubba F, Massimino D, Schwartz RA. Dermatoscopy: alternative uses in daily clinical practice. J Am Acad Dermatol. 2011; 64: 1135-46
11. Kittler H, Guitera P, Riedl E et al. Identification of clinically featureless incipient melanoma using sequential dermoscopy imaging. Arch Dermatol. 2006;142: 1113-9.
12. Tschandl P. Sequential digital dermatoscopic imaging of patients with multiple atypical nevi. Dermatol Pract Concept. 2018; 8: 231-237.
13. Wu X, Marchetti MA, Marghoob AA. Dermoscopy: not just for dermatologists. Melanoma Manag. 2015; 2:63-73.
14. Salerni G, Terán T, Puig S et al. Meta-analysis of digital dermoscopy follow-up of melanocytic skin lesions: a study on behalf of the International Dermoscopy Society. J Eur Acad Dermatol Venereol. 2013; 27: 805-14.
15. Dinnes J, Deeks JJ, Chuchu N et al. Dermoscopy, with and without visual inspection, for diagnosing melanoma in adults. Cochrane Database Syst Rev. 2018; 12: CD011902.

16. Giuffrida R, Conforti C, Resende FSS et al. Clinical and dermoscopic features of genital pigmented Bowen disease. Clin Exp Dermatol. 2018; 43: 813-6.

17. Fargnoli MC, Kostaki D, Piccioni A et al. Dermoscopy in the diagnosis and management of non-melanoma skin cancers. Eur J Dermatol. 2012; 22: 456-63.

18. Hamilko de Barros M, Conforti C, Giuffrida R et al. Clinical usefulness of dermoscopy in the management of lentigo maligna melanoma treated with topical imiquimod: A case report. Dermatol Ther. 2019; 32: e13048.

19. Giuffrida R, Borgia F, Cannavò SP. Two cases of erosive pustular dermatosis of the scalp occurring after topical 3.75% imiquimod for actinic keratoses. Dermatol Ther. 2019; 32: e12770.

20. Seabra Resende FS, Conforti C, Giuffrida R, et al. Balloon Cell Primary Nodular Melanoma: Dermoscopy Evidence. Dermatol Pract Concept. 2019; 9:155-6.

21. Drugge ED, Volpicelli ER, Sarac RM et al. Micromelanomas identified with time-lapse total body photography and dermoscopy. J Am Acad Dermatol. 2018; 78: 182-3.

22. Argenziano G, Kittler H, Ferrara G et al. Slow-growing melanoma: a dermoscopy follow-up study. Br J Dermatol. 2010; 162: 267-73.

23. Salerni G, Carrera C, Lovatto L et al. Benefits of total body photography and digital dermatoscopy ("two-step method of digital follow-up") in the early diagnosis of melanoma in patients at high risk for melanoma. J Am Acad Dermatol. 2012; 67: e17-27.
24. Pagnanelli G, Soyer HP, Argenziano G et al. Diagnosis of pigmented skin lesions by dermoscopy: web-based training improves diagnostic performance of non-experts. Br J Dermatol. 2003; 148: 698-702.
25. Ahlgrimm-Siess V, Laimer M, Rabinovitz HS et al. Confocal Microscopy in Skin Cancer. Curr Dermatol Rep. 2018; 7: 105-18.
26. Guida S, Longo C, Casari A et al. Update on the use of confocal microscopy in melanoma and non-melanoma skin cancer. G Ital Dermatol Venereol. 2015; 150: 547-63.
27. Farnetani F, Scope A, Coco V et al. Paradigmatic cases of pigmented lesions: How to not miss melanoma. J Dermatol. 2016; 43:1433-7.
28. Guida S, Pellacani G, Cesinaro AM, et al. Spitz naevi and melanomas with similar dermoscopic patterns: can confocal microscopy differentiate? Br J Dermatol. 2016; 174: 610-6.
29. Hibler BP, Qi Q, Rossi AM. Current state of imaging in dermatology. Semin Cutan Med Surg. 2016; 35: 2-8.

30. Schneider SL, Kohli I, Hamzavi IH et al. Emerging imaging technologies in dermatology: Part II: Applications and limitations. J Am Acad Dermatol. 2019; 80:1121-31.
31. Farnetani F, Manfredini M, Chester J et al. Reflectance confocal microscopy in the diagnosis of pigmented macules of the face: differential diagnosis and margin definition. Photochem Photobiol Sci. 2019;18: 963-9.
32. Moscarella E, Rabinovitz H, Zalaudek I et al. Dermoscopy and reflectance confocal microscopy of pigmented actinic keratoses: a morphological study. J Eur Acad Dermatol Venereol. 2015; 29: 307-14.
33. Dorrell DN, Strowd LC. Skin Cancer Detection Technology. Dermatol Clin. 2019; 37: 527-36.
34. Nguyen KP, Peppelman M, Hoogedoorn L et al. The current role of in vivo reflectance confocal microscopy within the continuum of actinic keratosis and squamous cell carcinoma: a systematic review. Eur J Dermatol. 2016; 26: 549-65.
35. Conforti C, Paolini F, Venuti A et al. The detection rate of human papillomavirus in well-differentiated squamous cell carcinoma and keratoacanthoma: is there new evidence for a viral pathogenesis of keratoacanthoma? Br J Dermatol. 2019; 181: 1309-11.

36. Lupu M, Popa IM, Voiculescu VM et al. A systematic review and meta-Analysis of the accuracy of in vivo reflectance confocal microscopy for the diagnosis of primary basal cell carcinoma. J Clin Med. 2019; 8. pii: E1462.
37. Segura S, Puig S, Carrera C. et al Development of a two-step method for the diagnosis of melanoma by reflectance confocal microscopy. J Am Acad Dermatol. 2009; 61: 216-29.
38. Wortsman X, Wortsman J. Clinical usefulness of variable-frequency ultrasound in localized lesions of the skin. J Am Acad Dermatol. 2010; 62: 247-56.
39. Maj M, Warszawik-Hendzel O, Szymanska E et al. High frequency ultrasonography: a complementary diagnostic method in evaluation of primary cutaneous melanoma. G Ital Dermatol Venereol. 2015; 150: 595-601.
40. Bakos RM, Blumetti TP, Roldán-Marín R, Salerni G. Noninvasive imaging tools in the diagnosis and treatment of skin cancers. Am J Clin Dermatol. 2018; 19: 3-14.
41. Reggiani C, Manfredini M, Mandel VD et al. Update on non-invasive imaging techniques in early diagnosis of non-melanoma skin cancer. G Ital Dermatol Venereol. 2015; 150: 393-405.

42. Wang J, Xu Y, Boppart SA. Review of optical coherence tomography in oncology. J Biomed Opt. 2017; 22: 1-23.

43. Welzel J, Schuh S. Noninvasive diagnosis in dermatology. J Dtsch Dermatol Ges. 2017;15: 999-1016.

44. Fink C, Haenssle HA. Non-invasive tools for the diagnosis of cutaneous melanoma. Skin Res Technol. 2017; 23: 261-271.

45. Mohr P, Birgersson U, Berking C et al. Electrical impedance spectroscopy as a potential adjunct diagnostic tool for cutaneous melanoma. Skin Res Technol. 2013; 19:75-83.

46. Malvehy J, Hauschild A, Curiel-Lewandrowski C et al. Clinical performance of the Nevisense system in cutaneous melanoma detection: an international, multicentre, prospective and blinded clinical trial on efficacy and safety. Br J Dermatol. 2014; 171:1099-107.

47. Braun RP, Mangana J, Goldinger S et al. Electrical Impedance Spectroscopy in Skin Cancer Diagnosis. Dermatol Clin. 2017; 35: 489-493.

48. Hartinger AE, Guardo R, Kokta V, Gagnon H. A 3-D hybrid finite element model to characterize the electrical behavior of cutaneous tissues. IEEE Trans Biomed Eng. 2010; 57: 780-9.

49. Zhao J, Zeng H, Kalia S, Lui H. Using Raman Spectroscopy to Detect and Diagnose Skin Cancer In Vivo. Dermatol Clin. 2017; 35: 495-504.

50. Lui H, Zhao J, McLean D, Zeng H. Real-time Raman spectroscopy for in vivo skin cancer diagnosis. Cancer Res. 2012; 72: 2491-500.

CHAPTER 2

Clinical and dermoscopic characteristics of nevus-associated melanomas

(Zalaudek I, Conforti C, Guarneri F, Vezzoni R, Deinlein, Hofmann-Wellenhof R, Longo C, Moscarella E, Kittler H, Argenziano G, Giuffrida R. JAAD under revision)

INTRODUCTION

The "traditional" model of melanoma progression suggests that this tumor develops through a stepwise malignant transformation process, from a common nevus to a dysplastic nevus and, finally, to melanoma in situ, which eventually becomes invasive with the potential to metastasize.[1,2] Mounting evidence contradicts this model as most melanomas develop de novo, while only a negligible number of nevi will ever progress towards melanoma. Moreover, when melanoma arises in a pre-existing nevus, the associated nevus will turn out, in most cases, to be a banal nevus, often showing congenital-like features and no evidence of "dysplastic" features.[3,4] As a consequence, this model is increasingly abandoned by clinicians and researchers.

There is no doubt that a certain proportion of melanomas may arise within a nevus. The most well documented risk of malignant transformation belongs to large congenital melanocytic nevi, whereas the risk of small congenital nevi and acquired nevi is not well defined and less well documented.[5] According to histopathological studies, about 30% of melanomas arise in

association with a nevus.[6] It must be admitted, however, that this number does not reflect the true frequency of the event as histopathologic studies rely on selection bias and refer only to lesions that have been excised. Real life estimations suggest that the annual transformation rate of a single nevus into melanoma ranges from 0.0005% or less (i.e. 1 in 200.000) under the age of 40 years, to 0.003% (about 1 in 33.000) in persons older than 60 years.[7] Thus, the calculated risk of any particular nevus becoming melanoma is exceedingly low. Dermoscopy improves the early diagnosis of melanoma and categorization of nevi compared to the naked eye and there are multiple studies focusing on the dermoscopic patterns or melanomas and nevi. In contrast, there is only little known about the clinical and dermoscopic criteria of nevus-associated melanoma (NAM).[8,9] The aim of this retrospective morphological study was to gain insights into the morphological spectrum of nevi associated with melanomas and vice versa.

MATERIAL AND METHODS

This retrospective, morphological study involved dermatological clinics in Austria (Graz, Vienna) and Italy (Messina, Napoli, Reggio Emilia, Trieste). The protocol of the study was approved by the Local Institutional Review Board.

Each participating center searched its database for clinical and dermoscopic images of histopathologically diagnosed NAM. Each included case was assigned to an identification number in order to guarantee anonymization of sensitive patients' data. After anonymization, clinical and dermoscopic images were formatted into powerpoint or keynote files, which were sent via email along with an excel file containing identification number, patients' age, gender, tumor location, clinical diameter and, if available, histopathologically reported nevus component and Breslow thickness of the melanoma to the collecting center.

There were no pre-requisites regarding the technical device used to obtain the clinical and dermoscopic photographs. Cases with a missing according clinical or dermoscopic image, or for which the clinical or dermoscopic photographs showed only tumor parts as well as images with poor quality were excluded from the study.

All clinical and dermoscopic images were reviewed by 4 dermatologists with >5 years of experience in dermoscopy (IZ, RG, EM, CL) and evaluated for pre-defined clinical and dermoscopic criteria. The analysis was made in consensus between the evaluators. If no consensus was reached, the criterion was scored as absent.

The evaluation was in based on 3 mains 'funnel questionnaires', which requested a trichotomous (yes/no/unsure) answer (Figure 2.1). The first

question verified whether a nevus component was clinically visible. Only if the answer was “yes” or “unsure”, the further subsequent evaluations were required. The second question was about the presence of a dermoscopically recognizable nevus component. If the question was answered with “yes” or “unsure”, the further items were evaluated. If neither clinically nor dermoscopically a nevus component was detected, the evaluation immediately proceeded to question 3, which aimed to assess melanoma-specific patterns.

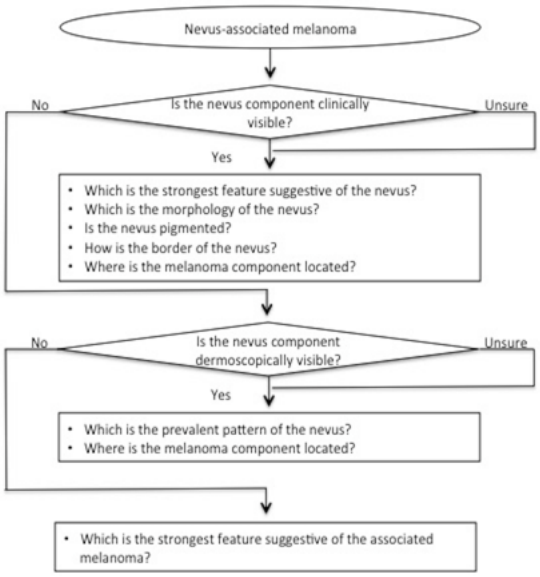

Figure 2.1. Schematic illustration of the 3 mains ‘funnel questionnaire’ used for the clinical and dermoscopic evaluation of nevus-associated melanoma.

Statistical analysis

Results were expressed as mean and standard deviation, minimum and maximum in case of continuous variables, or as absolute frequency and percentage in case of qualitative variables. Differences of frequency between subgroups were evaluated using the Mann-Whitney test for continuous variables and the chi square test or Fisher's exact test, as appropriate, for qualitative variables, and $p<0.05$ was considered significant. Calculations were performed using Microsoft Excel (Microsoft, Redmond, USA) with the Real Statistics Resource Pack addin software (http://www.real-statistics.com).

RESULTS

General results

We included 165 patients (94 males, 56.97%, mean age 47.64±17.20 years, range 10-89) with 165 NAMs. The most frequent location of NAMs was the upper back (31.52%), followed by mid-lower back (16.97%), upper arms (13.33%), lower extremities (10.91%), abdomen (8.48%), chest (8.48%) and head/neck area (7.88%); other sites were affected in the remaining 2.42%. Mean clinical size of the lesions was 11.68±12.12 mm (range 3 to 150 mm).

Clinical features

Clinically, a nevus component was not recognized in 85 cases (51.52%) and recognizable in 80 (48.48%). Of the latter, a nevus was clearly seen in 69 (86.25%) and likely seen in 11 (13.75%). The strongest feature suggestive of a nevus was the simultaneous presence of two different morphologic clones, which was present in 46 (57.5%) cases, followed by different colors in 28 cases (35%), terminal hairs in 4 (5%) and overall size in 2 (2.5%) cases. The associated nevus was flat in 33 cases (41.25%), papular in 22 (27.5%), nodular in 16 (20%), papillomatous in 9 (11.25%). Fifty-five nevi (68.75%) were pigmented. Borders were sharply demarcated in 55 cases (68.75%) and ill-defined in the remaining 25 (31.25%).

Of note, the melanoma component arose adjacent (eccentric/peripheral) to the associated nevus in 45 (56.25%) cases, while was located central within the nevus in 35 (43.75%) (Figure 2.2).

Dermoscopic features

Dermoscopy revealed a nevus component in 89 cases (53.94%), while in 22 (13.33%) cases the nevus was considered likely; no dermoscopic evidence of nevus was present in the remaining 54 (32.73%).

In the overall 111 (67.27%) cases in which a nevus component was dermoscopically visible, the prevalent features were, in decreasing order of

frequency: regular dots/clods (n=31, 27.93%), structureless brown areas (n=28, 25.23%), typical pigmented network (n=22, 19.82%), hypopigmented structureless areas (n=15, 14.41%), central hypopigmented/hyperpigmented structureless areas surrounded by peripheral reticular pattern (n=9, 8.11%), hairs (n=3, 2.7%), streaks (n=1, 0.9%) and structureless blue areas (n=1, 0.9%). Dermoscopically, the melanoma was eccentric/peripheral in 59 cases (53.15%), central in 52 (46.85%) (Figure 2.2).

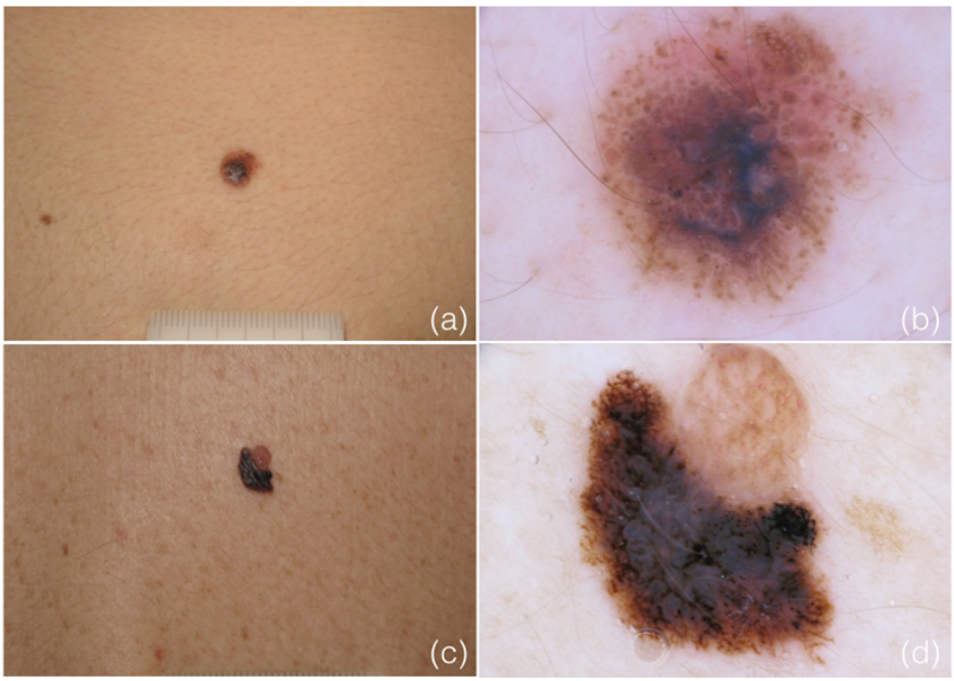

Figure 2.2. Clinical and dermoscopic appearance of two nevus-associated melanomas (NAMs). a-b) Melanoma arising within a nevus of congenital type and c-d) adjacent to an acquired nevus.

Melanoma identification in NAMs was based on various dermoscopic criteria, including atypical network, irregular dots/globules, streaks,

regression, raised blue color, reticular depigmentation, melanoma-associated vascular structures, atypical blotches, structureless brown and shiny white structures. In the majority of cases (90/165, 54.5%), dermoscopy showed the simultaneous presence of two or more criteria in the same lesion (multicomponent lesions), while in the others only one criterion was observed.

Histopathologic features

Histologically, the reported associated nevus was referred as nevus of the congenital type in 47 cases (28.48%), non-congenital in 118 (71.52%); this latter category included 59 (50%) compound nevi, 34 (28.81%) dysplastic nevi, 24 (20.34%) dermal nevi and one blue nevus (0.85%).

Mean Breslow thickness of all melanomas was 0.53±0.70 mm (range: 0 to 5.3 mm); in detail, there were 55 (33.3%) in situ melanomas, 89 (53.9%) melanomas with <1 mm thickness, 15 melanomas (9.1%) with thickness between 1 and 2 mm. Only 6 (3.6%) were more than 2 mm in thickness.

Comparison of melanomas arising in nevi with congenital features (C-NAM) versus nevi without congenital features (NC-NAM)

We compared the demographics and lesion characteristics of patients with melanomas associated with congenital nevi (C-NAM) with those having

melanomas associated with nevi without congenital features (NC-NAM). No differences between the two groups were seen for gender (23 males and 24 females with C-NAMs vs 71 males and 47 females with NC-NAMs, p=0.19), location of the melanomas (p=0.95) or mean size (15.13±21.33 mm for C-NAM vs 10.31±4.53 mm for NC-NAM, p=0.19). Patients with histopathological C-NAM were significantly younger compared to those with histopathological NC-NAM (39.02±17.63 vs 51.08±15.84 years, p=0.0001). Breslow thickness was significantly greater (p=0.047) in C-NAMs (0.70±0.92 mm) than in NC-NAMs (0.46±0.58 mm).

In patients with a clinically visible nevus component, significant differences were found for age (40.62±18.3 years for C-NAM patients vs 48.69±14.65 years for NC-NAM patients, p=0.039), nevus associated features (p=0.048, see Table 2.1 for details), nevus pigmentation (25/26 pigmented C-NAMs vs 30/54 NC-NAMs, p=0.00014), nevus borders (sharp in 22/26 C-NAMs vs 33/54 NC-NAMs, p=0.03). A significant difference between the two groups concerned also the melanoma localization, which was central in the majority of C-NAMs (20/26, 76.92%) and eccentric/peripheral in the majority of NC-NAMs (39/54, 72.22%; p=0.00003). No significant differences between the groups were seen for gender distribution (p=0.76), nor for location (p=0.79), size (p=0.29), Breslow thickness (p=0.11) or morphology (p=0.24) of lesions.

Table 2.1. Clinically and dermoscopically visible features of the nevus component of nevus-associated melanomas (NAMs), congenital (C-NAM) and non-congenital (NC-NAM).

	No. of NAMs with the features indicated		*p*
	C-NAM	NC-NAM	
Clinical features			
Size	2 (7.69%)	0 (0%)	0.051
Color	8 (30.77%)	20 (37.04%)	0.58
Terminal hairs	3 (11.54%)	1 (1.85%)	0.054
Two different components	13 (50%)	33 (61.11%)	0.35
Overall			***0.048***
Dermoscopic features			
Regular dots/globules	16 (44.44%)	15 (20%)	**0.007**
Typical pigmented network	5 (13.89%)	17 (22.67%)	0.28
Structureless brown	10 (27.78%)	18 (24%)	0.67
Hypopigmented structureless	1 (2.78%)	15 (20%)	**0.014**
Central structureless + peripheral reticular	3 (8.33%)	6 (8%)	0.86
Streaks	0 (0%)	1 (1.33%)	0.66
Structureless blue	1 (2.78%)	0 (0%)	0.16
Hairs	0 (0%)	3 (4%)	0.4
Overall			***0.032***

Similarly, patients with a dermoscopically visible nevus component revealed significant differences with regard to age (35.92±18.2 years for C-NAM patients vs 48.79±15.88 years for NC-NAM patients, p=0.0003) and dermoscopic pattern of the nevus component (p=0.032, see Table 2.1). In detail, C-NAMs revealed significantly more frequent regular dots/globules (p=0.007), while hypopigmented structureless areas were prevalent in NC-NAMs (p=0.014). No differences were seen for gender (p=0.39), nor location (p=0.88), size (p=0.38) and Breslow thickness (p=0.20) of lesions.

Notably, the most evident difference between the two groups concerned the localization of melanomas with regard to the nevus. While the majority of C-

NAMs (28/36, 77.78%) exhibited a central melanoma component, 51 out of 75 NC-NAMs (68%) displayed an eccentric/peripheral melanoma component (p=0.000006).

However, we noticed that the melanoma component of any NAM, independent from the subgroup, tended to be more frequently central in patients aged ≤40 years and eccentric/peripheral in those >40 years. Data from clinical observation showed such trend, close to statistical significance (p=0.06), which was confirmed at dermoscopic examination (p=0.0017).

Finally, we performed a comparison between the frequency of dermoscopic features of C-NAMs and NC-NAMs. Results are shown in Table 2.2.

Table 2.2. Frequency of dermoscopic features of nevus-associated melanoma (NAMs), congenital (C-NAMs) and non-congenital (NC-NAMs).

Dermoscopic features	Occurrences in C-NAMs			Occurrences in NC-NAMs			p values for occurrences in C-NAMS vs NC-NAMs		
	Single-component	Multi-component	Total	Single-component	Multi-component	Total	Single-component	Multi-component	Total
Atypical network	6	11	17	20	55	75	0.09	**0.036**	**0.001**
Irregular dots/globules	1	10	11	3	30	33	0.64	0.57	0.55
Streaks	0	2	2	2	11	13	0.28	0.52	0.17
Regression	9	18	28	5	62	77	**0.014**	0.86	0.94
Raised blue color	5	0	5	2	0	2	**0.040**	n/a	**0.010**
Reticular depigmentation	0	5	5	2	14	16	0.28	0.63	0.61
Melanoma-associated vascular structures	1	3	4	4	20	24	0.44	0.22	0.07
Atypical blotches	1	0	1	3	0	3	0.64	n/a	0.88
Structureless brown	3	0	3	7	0	7	0.67	n/a	0.91
Shiny white structures	1	6	7	0	20	20	0.18	0.90	0.75
Overall							0.07	0.84	0.12

DISCUSSION

Our study confirms current data with regard to the epidemiology of NAMs but opens also novel insights into their morphologic variability, which suggest different pathways leading to melanoma formation in nevi.

In line with previous studies,[10] NAMs in our study were associated with an average age around the 5th decade of life, slightly more frequent in men (57%) and mainly located on upper to mid-lower back and upper extremities, while being rarely on the head/neck area or lower extremities. Also, in agreement with current literature, the most frequent reported nevus types associated with NAM in our study were congenital, compound and dermal nevi with or without dysplasia,[3,4] while junctional or lentiginous nevi appear nearly exclusive for the development of NAM. This might be related to the histopathological difficulties to accurately differentiate the junctional component of a nevus from that of an associated melanoma. However, it must be admitted that this hypothesis does not explain why NAM, according to the current literature, occur at younger age compared to de novo melanomas.[11] Our study shows that, although NAMs in our study presented an average diameter of 11.68±12.12 mm, an associated nevus was clinically recognizable in only about 48% of cases. The most suggestive criteria for an associated nevus were different morphologic components and colors between the nevus and melanoma component, whereby the associated nevus

revealed a raised to nodular shape. Dermoscopy improved the recognition of an associated nevus up to 67% of cases, whereby regular globules/clods, structureless brown areas and a regular network were the most frequent criteria associated with the nevus. With regard to melanoma-specific features in NAMs, Shitara et al.[12] reported the presence of a negative pigment network (reticular depigmentation), globules and streaks as surrogate criteria for the diagnosis of NAM; in our analysis, however, only irregular globules being frequent in NAM, while reticular depigmentation and streaks were rarely observed in our series.

A key finding of our study, to the best of our knowledge not previously reported, is related to the location of melanomas developing in association with a nevus. We observed two main patterns of NAM: melanomas arising centrally and eccentrically in relation to the nevus. The first pattern was associated with younger age (<40 years) and nevi showing congenital-like features, both dermoscopically (globular pattern) and histopathologically. Instead, the latter pattern occurred more frequently in older individuals in raised to nodular hypopigmented nevi (mainly compound or dermal nevi) without reported congenital features. Moreover, NC-NAMs revealed an atypical network more often than C-NAMs. This can be explained by the fact that NC-NAMs were on average thinner than C-NAMs (0.46±0.58 vs 0.70±0.92 mm). In turn, NC-NAMs may be related to an earlier recognition

of melanomas developing adjacent to a nevus, which cause a more pronounced clinical asymmetry of the overall gestalt compared to melanomas which arise within a nevus without affecting initially its overall symmetric shape.

The epidemiological, demographic and morphological differences between melanomas arising within and adjacent to the nevus point furthermore towards two different pathways of melanoma development in nevi, namely within “congenital” and adjacent to “acquired” nevi (Figure 2.3).

This is in line with the current dermoscopic concept of nevogenesis, which also postulates that nevi develop via a congenital and acquired pathway.[13-15] According to the dual concept of nevogenesis, the congenital pathway gives rise to nevi with a clod/globular or structureless brown pattern, which may be present at birth (true small congenital nevi) or develop during early childhood (late small congenital nevi) and persists throughout lifetime. Studies suggest that such nevi are particularly commonly observed on the upper torso of children with a fair pigmentary trait.[16] In line with this, clods/globules or structureless brown pigmentation were a common finding in our series of C-NAMs. In this nevus type, melanoma appears to develop overlying in the center of the nevus.

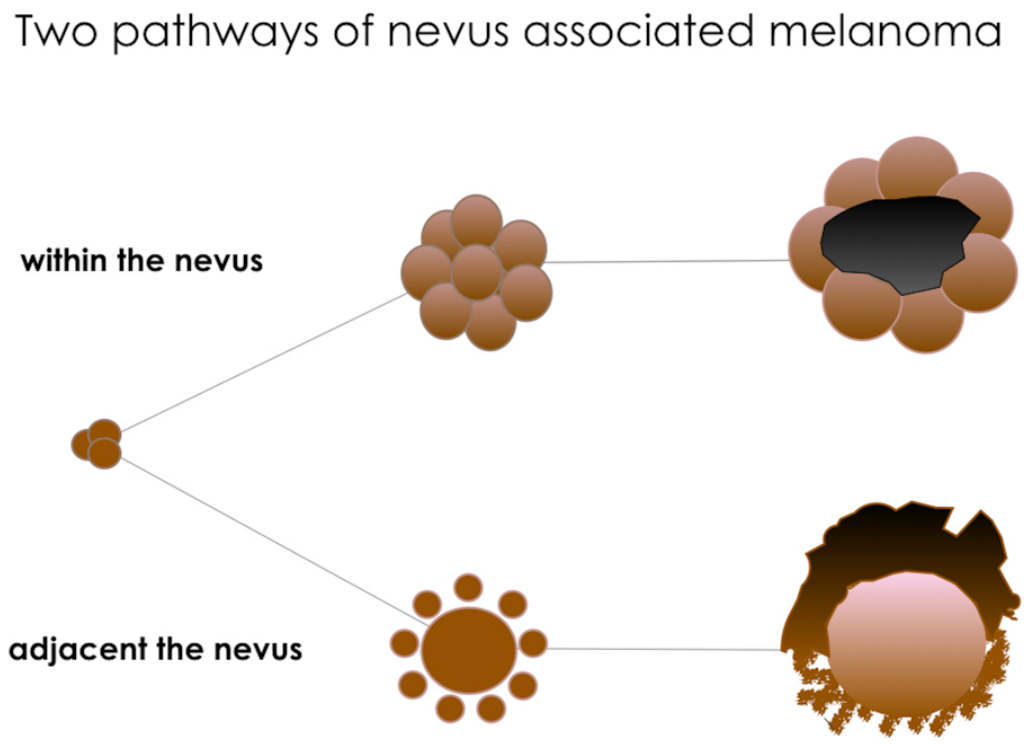

Figure 2.3. Model illustrating two different pathways of melanoma development in nevi, namely within "congenital" and adjacent to "acquired" nevi.

Instead, the second pathway leads to the formation of nevi that develop after puberty and are initially characterized by a peripheral rim of brown globules,[17] and later develop into nevi with a prevalent reticular (superficial compound) or reticular mixed pattern (deep compound).[18] Although the majority of these "acquired" nevi will undergo spontaneous involution after the 4-5th decade of life,[19] it is plausible that in some deep compound nevi (often with a fried egg appearance), characterized by a hypopigmented structureless elevated center (corresponding to the deep dermal component)

and peripheral flat network (corresponding to the lateral junctional shoulders), the central dermal component persists for a longer period. In these nevi, melanoma appears to develop adjacent to the nevus.

In this context, it appears particularly interesting that Pandeya et al. [20] recently reported the association of NAMs with blue and green eyes (i.e., a fair pigmentary trait), and also nevi with a clod/globular pattern or central hypopigmentation have been associated to a fair pigmentary trait. [21] Despite this, they found a higher frequency of $BRAF^{V600E}$ compared to de novo melanomas, leading them to speculate whether $BRAF^{V600E}$ plays a role in the pathogenesis of NAM. In fact, $BRAF^{V600E}$ is widely considered an initial driver event in melanoma progression, while the same mutation in nevi appears to play a role as driver event only initially, and later instead causes growth arrest via oncogen-driven senescence.[22] Our group was the first to show that the frequency of $BRAF^{V600E}$ in nevi depends on the clinical, dermoscopic and histopathological morphology and growth stage of a given nevus. As such, we found the highest mutational frequency among nevi with a dermoscopic globular/clod pattern, while the frequency in compound nevi (reticular, reticular mixed pattern) appeared growth dependent, i.e. high during active growth and decreasing at growth arrest.[22] Tschandl et al.[23] investigated the frequency of $BRAF^{V600E}$ and NRAS mutations in the nevus and melanoma components of the same NAM, but found no correlation

between the nevus and melanoma components with regard to the mutational status. Based on this, they concluded that $BRAF^{V600E}$ seems to play no role in the progression of melanoma arising with a nevus; however, they did not mention whether melanomas arose within or adjacent to the nevus in their study. Future studies investigating the frequency of $BRAF^{V600E}$ considering the location of melanoma within the nevus and subtype of the nevus may shed more light on this.

Our study has several limitations. First, we retrospectively collected cases, and therefore no further information about additional patients' characteristics such as nevus count, eye color or skin type can be provided. Second, in our analysis we relied on the reported routine histopathological diagnosis of the associated nevus and did not perform a review of the histopathological slides. Thus, no conclusions about the interobserver agreement of the histopathological characteristics of the associated nevus can be provided. Third, the evaluation of specific criteria between the associated nevus and melanoma were based on the clinical and dermoscopic assumption of the associated components and not on a clinical-histopathological correlation. However, assessment of whether a component was related to the nevus or the melanoma was performed in consensus and on the according dermoscopic criteria. Finally, we did not perform any molecular tests with

regard to the frequency of BRAF or NRAS of the associated nevi and melanomas in our series.

In summary, our study reveals two types of NAMs, namely melanomas arising within/overlying congenital nevi, characterized by a clod/globular or structureless brown pattern, and melanomas arising adjacent to acquired nevi, appearing more frequently as hypopigmented nodules or plaques. Persons developing the former type are generally younger compared to the latter subtype. In the latter subtype, the adjacent location appears to facilitate the early recognition of melanoma compared to the former. However, as no current method allows to predict which nevus will develop melanoma, prophylactic excision of these common nevi is not recommended. This recommendation should be also seen in the light of a considerably low overall risk of progression.

REFERENCES

1. Bastian BC. The molecular pathology of melanoma: an integrated taxonomy of melanocytic neoplasia. Annu Rev Pathol. 2014; 9: 239-71.
2. Liu V, Mihm MC. Pathology of malignant melanoma. Surg Clin North Am. 2003; 83: 31-60.
3. Alendar T, Kittler H. Morphologic characteristics of nevi associated with melanoma: a clinical, dermatoscopic and histopathologic analysis. Dermatol Pract Concept. 2018; 8: 104-8.
4. Kaddu S, Smolle J, Zenahlik P, Hofmann-Wellenhof R, Kerl H. Melanoma with benign melanocytic naevus components: reappraisal of clinicopathological features and prognosis. Melanoma Res. 2002; 12: 271-8.
5. Krengel S, Hauschild A, Schäfer T. Melanoma risk in congenital melanocytic naevi: a systematic review. Br J Dermatol. 2006; 155:1-8.
6. Pampena R, Kyrgidis A, Lallas A, Moscarella E, Argenziano G, Longo C. A meta-analysis of nevus-associated melanoma: prevalence and practical implications. J Am Acad Dermatol. 2017; 77: 938-45.e4.
7. Tsao H, Bevona C, Goggins W, Quinn T. The transformation rate of moles (melanocytic nevi) into cutaneous melanoma: a population-based estimate. Arch Dermatol. 2003; 139:282-8.

8. Alvarez Martinez D, Boehncke WH, Kaya G, Merat R. Recognition of early melanoma: a monocentric dermoscopy follow-up study comparing de novo melanoma with nevus-associated melanoma. Int J Dermatol. 2018; 57: 692-702.
9. Stante M, Carli P, Massi D, de Giorgi V. Dermoscopic features of naevus-associated melanoma. Clin Exp Dermatol. 2003; 28: 476-80.
10. Bevona C, Goggins W, Quinn T, Fullerton J, Tsao H. Cutaneous melanomas associated with nevi. Arch Dermatol. 2003; 139: 1620-4.
11. Cymerman RM, Shao Y, Wang K, Zhang Y, Murzaku EC, Penn LA et al. De novo vs nevus-associated melanomas: differences in associations with prognostic indicators and survival. J Natl Cancer Inst. 2016; 108: djw21.
12. Shitara D, Nascimento M, Ishioka P, Carrera C, Alós L, Malvehy J et al. Dermoscopy of naevus-associated melanomas. Acta Derm Venereol. 2015; 95: 671-5.
13. Zalaudek I, Catricalà C, Moscarella E, Argenziano G. What dermoscopy tells us about nevogenesis. J Dermatol. 2011; 38: 16-24.
14. Pellacani G, Scope A, Ferrari B, Pupelli G, Bassoli S, Longo C et al. New insights into nevogenesis: in vivo characterization and follow-up of melanocytic nevi by reflectance confocal microscopy. J Am Acad Dermatol. 2009; 61: 1001-13.

15. Woltsche N, Schmid-Zalaudek K, Deinlein T, Rammel K, Hofmann-Wellenhof R, Zalaudek I. Abundance of the benign melanocytic universe: Dermoscopic-histopathological correlation in nevi. J Dermatol. 2017; 44: 499-506.
16. Scope A, Marghoob AA, Chen CS, Lieb JA, Weinstock MA, Halpern AC. Dermoscopic patterns and subclinical melanocytic nests in normal-appearing skin. Br J Dermatol. 2009; 160: 1318-21.
17. Kittler H, Seltenheim M, Dawid M, Pehamberger H, Wolff K, Binder M. Frequency and characteristics of enlarging common melanocytic nevi. Arch Dermatol. 2000; 136: 316-20.
18. Zalaudek I, Schmid K, Marghoob AA et al. Frequency of dermoscopic nevus subtypes by age and body site: a cross-sectional study. Arch Dermatol. 2011; 147: 663-70.
19. Zalaudek I, Grinschgl S, Argenziano G et al. Age-related prevalence of dermoscopy patterns in acquired melanocytic naevi. Br J Dermatol. 2006; 154: 299-304.
20. Pandeya N, Kvaskoff M, Olsen CM et al. Factors related to nevus-associated cutaneous melanoma: a case-case study. J Invest Dermatol. 2018; 138: 1816-24.

21. Zalaudek I, Argenziano G, Mordente I et al. Nevus type in dermoscopy is related to skin type in white persons. Arch Dermatol. 2007; 143: 351-6.

22. Zalaudek I, Guelly C, Pellacani G et al. The dermoscopical and histopathological patterns of nevi correlate with the frequency of BRAF mutations. J Invest Dermatol. 2011; 131: 542-5.

23. Tschandl P, Berghoff AS, Preusser M et al. NRAS and BRAF mutations in melanoma-associated nevi and uninvolved nevi. PLoS One. 2013; 8: e69639.

CHAPTER 3

Dermoscopic findings in the presurgical evaluation of basal cell carcinoma. A prospective study.

(Giuffrida R, Conforti C, Zalaudek I, Guarneri F, Cannavò SP, Pizzichetta MA, Bonin S, Bussani R, Bazzacco G, Di Meo N. JEADV. Under revision)

INTRODUCTION

Dermoscopy has become an indispensable noninvasive tool for the dermatologist when evaluating skin cancers.[1,2] Its accuracy for the diagnosis of basal cell carcinoma (BCC) compared with examination with the naked eye has been well studied.[1,3,4] Indeed, it provides valuable information on the histopathological subtype, ensures a more accurate assessment of the tumor extension, allows the identification of pigmentation and other structures not visible to unaided eye and guides the clinician in the therapeutic choice.[1]

The goal of therapy for patients with BCC is the complete surgical removal of the tumor, in order to reduce local recurrences and minimize the aesthetic impact of the resulting scar, especially in the most sensitive cosmetic areas (e.g. the face).[5,6] Radical removal can be achieved either with clinical evaluation of safety margins or with micrographic control.[5]

Mohs' micrographic surgery (MMS) is a specialized surgical technique that enables complete and precise removal of skin tumor through microscopic margin analysis by using horizontal frozen sections.[7] Although MMS offers

undoubted advantages (it guarantees a high healing rate and preserves most healthy tissues), it is a complex, time-consuming and labor-intensive process.[7] Moreover, it is performed in few dermatologic centers, because it requires the expertise of qualified and trained surgeons, histology technician and nursing staff.[8]

This explains why traditional surgical excision is still widely used in the treatment of previously untreated BCC; it is a simpler, less costly and time-saving technique.[6]

The reported rate of incomplete surgical excision of BCC varies widely in literature, ranging between 4.7 and 24%.[6] This eventuality may be followed by recurrence of the tumor, that has been shown to be higher in case of margin involvement.[9,10]

An adequate presurgical evaluation of the tumor margins is then crucial, in order to avoid local recurrences.

For this purpose, different methods have been proposed, but dermoscopy has rarely been used.[11,12]

The aim of this study was to assess whether dermoscopy can detect the borders in BCCs more accurately than clinical evaluation alone and to describe the most common dermoscopic findings in the surrounding skin of clinically detected BCCs. In addition, dermoscopy was used in the

presurgical evaluation of removals, orienting the surgery in order to achieve oncological radicality.

MATERIAL AND METHODS

From October 2018 to May 2019, patients of Caucasian ethnicity, with clinical and dermoscopic suspicion of BCC, were enrolled for a traditional surgical excision. Sex, age, body location of the lesion and maximum diameter expressed in millimeters were recorded. The study was carried out according to the principles of "good clinical practice", in line with the Declaration of Helsinki on clinical studies, and was approved by the local Research Ethics Committee. Written informed consent was obtained from each participant.

Before surgery, each lesion was examined both clinically and dermoscopically by two dermatoscopists with more than 10 years of experience (IZ, NM). (Figures 3.1 and 3.2), in order to delineate the correct site of surgical incision.

The dermoscopic analysis was performed with a digital dermoscope (DermLite 3Gen) with polarized light.

Margins were defined using a dermographic pencil. In Figure 3.3, margins assessed with naked eye are demarcated in blue, while those evaluated under dermoscopy are drawn in red.

Figure 3.1. Clinical image of a nodular basal cell carcinoma localized on the arm.

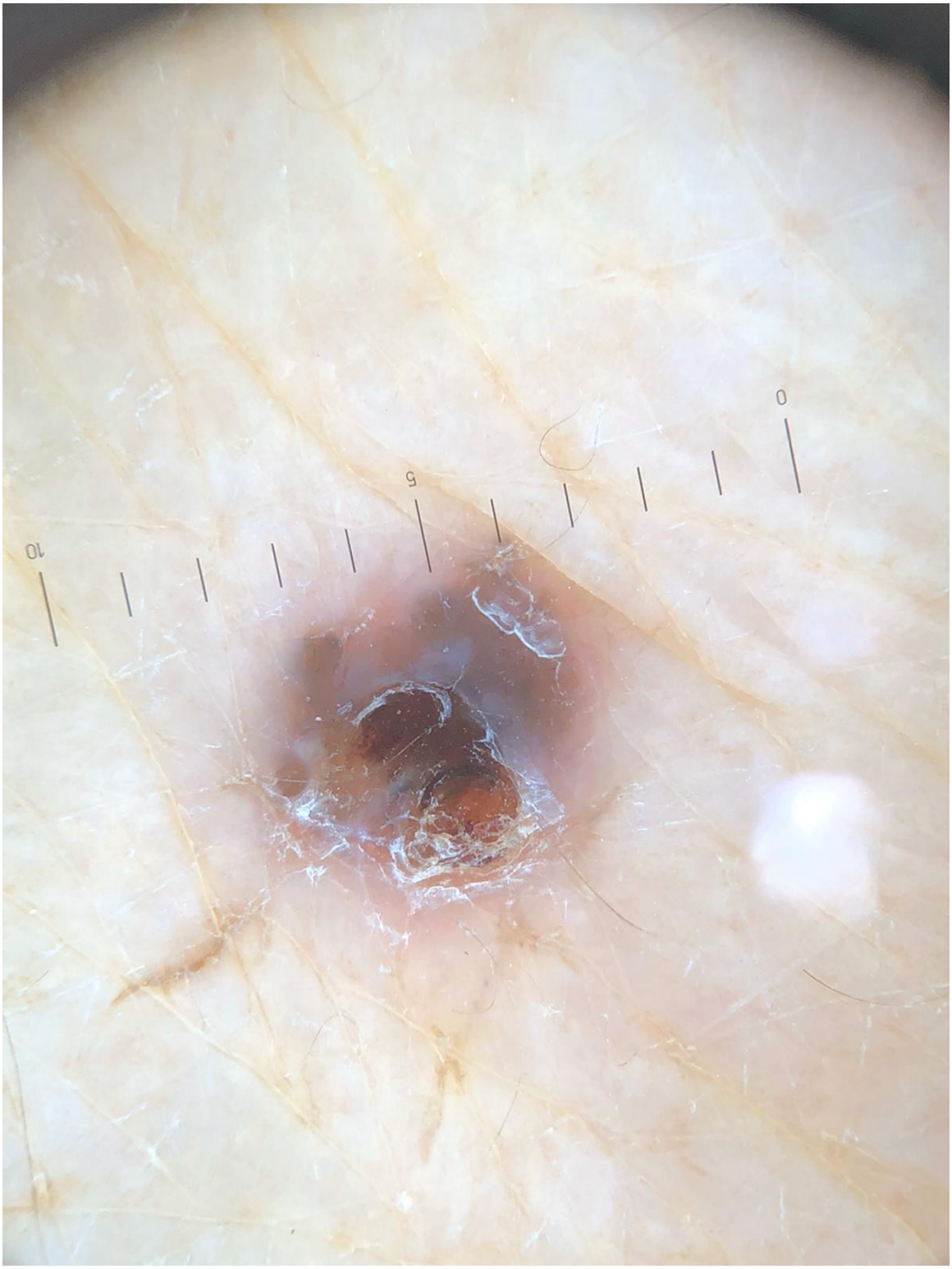

Figure 3.2. Dermoscopic picture of the nodular basal cell carcinoma illustrated in Figure 1.

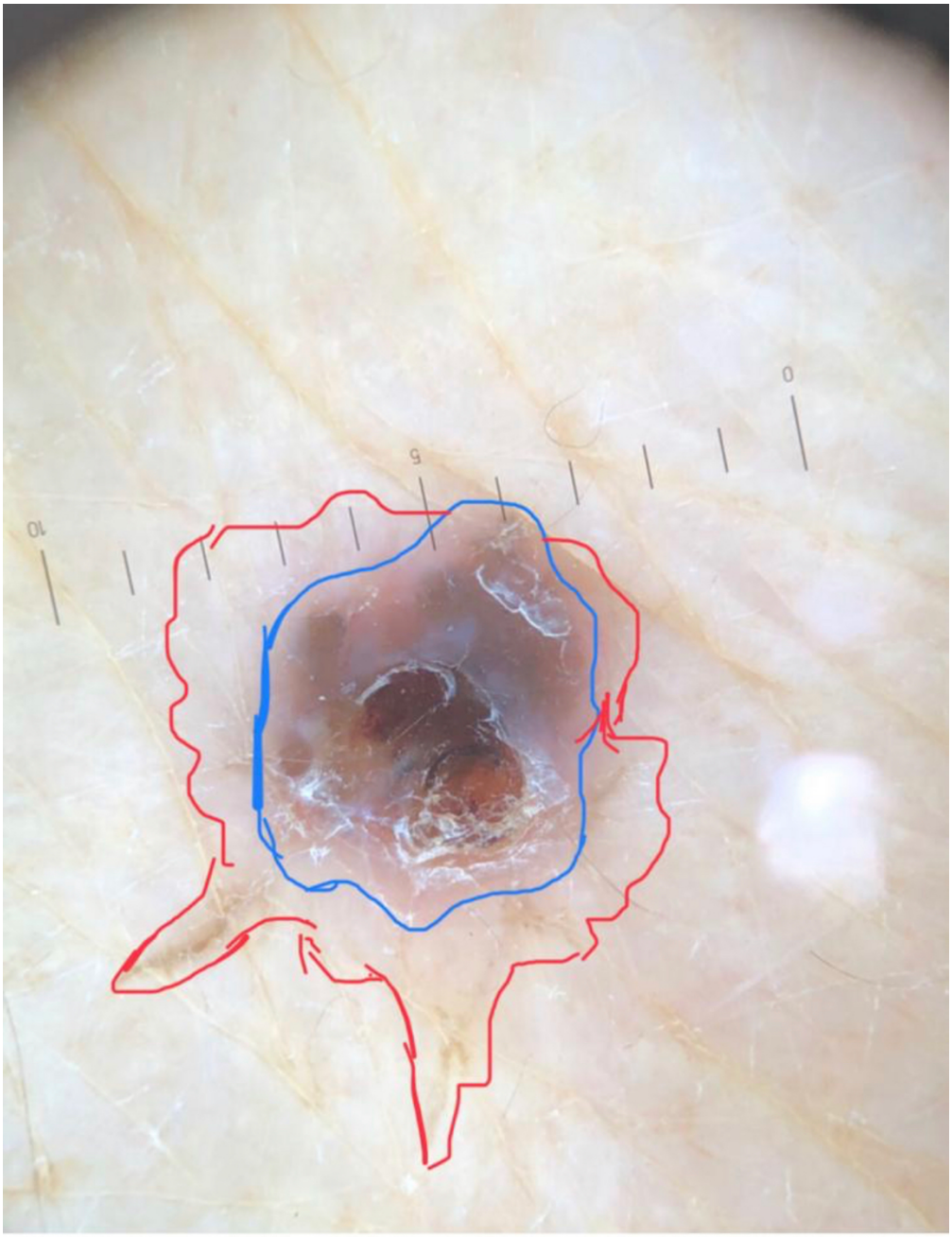

Figure 3.3. Dermoscopic picture of nodular basal cell carcinoma of the arm. Margins assessed with naked eye are demarcated in blue, while those evaluated under dermoscopy are drawn in red. The area between clinically and dermoscopically defined margins shows leaf-like areas (white arrows) and pink-white areas (black arrows). The purple arrow identifies a leaf-like area (collision with a superficial basal cell carcinoma?).

For each lesion, specific dermoscopic features have been searched in the skin adjacent to the demarcated clinical margin, including classical

(ulceration, multiple blue-gray globules, leaf-like areas, large blue-gray ovoid nests, spoke-wheel areas, arborizing vessels) and non-classical (short fine superficial telangiectasias, multiple small erosions, concentric structures, multiple in-focus blue-gray dots, shiny pink white areas, blue-whitish veil, milia like cysts) criteria for BCC.

Surgical treatment was performed following dermoscopic margins. Any difference between clinical and dermoscopic margins was recorded.

The samples obtained were histologically examined using haematoxylin and eosin staining and margins were classified as disease-free or disease-involved (Figure 3.4).

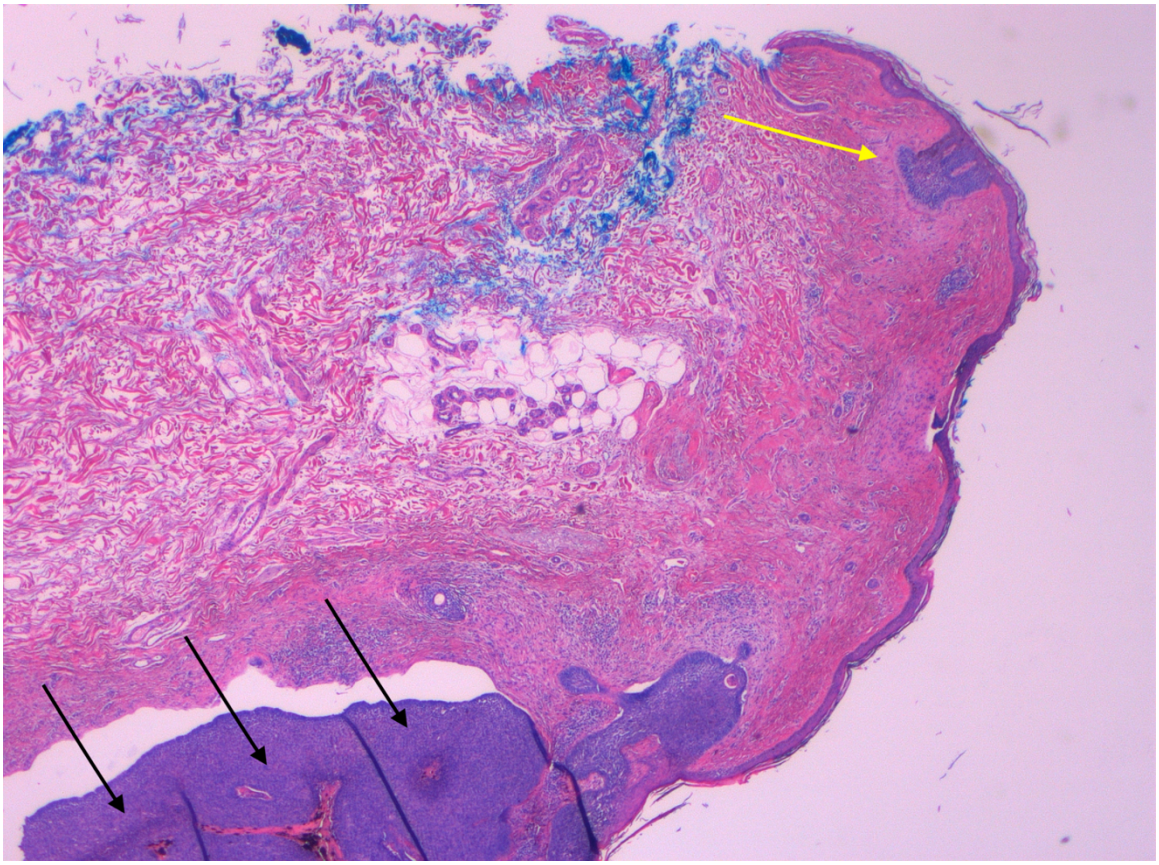

Figure 3.4. Hematoxylin-eosin-stained specimen corresponding to nodular basal cell carcinoma described in the previous figures (black arrows). The yellow arrow identifies a collision with a superficial basal cell carcinoma.

Statistical Analysis

Results were expressed as mean and standard deviation, minimum and maximum in case of continuous variables, or as absolute frequency and percentage in case of qualitative variables. Differences of frequency between subgroups were evaluated using the chi square test or Fisher's exact test, as appropriate, for qualitative variables, and $p<0.05$ was considered significant. Calculations were performed using Microsoft Excel (Microsoft, Redmond,

USA) with the Real Statistics Resource Pack addin software (http://www.real-statistics.com).

RESULTS

The study included 88 patients (51 males and 37 females) with a lesion having clinical-dermoscopic features of BCC. Mean age was 72.8±10.9 years, (range 27-95). Twenty-seven lesions (30.7%) were located in the head-neck region, 12 (13.6%) in the upper limbs, 3 (3.4%) in the lower limbs, 42 (47.7%) in the thorax and 4 (4.5%) in the abdomen. The maximum diameter of the lesions examined was between 3 and 40 mm (mean 9.4 ± 5.7 mm).

At histology 51 (58%) BCCs were nodular, 27 (30.7%) superficial, 3 (3.4%) pigmented, 2 (2.3%) sclerodermiform, 1 (1.1%) follicular, 1 (1.1%) adenoid-cystic and 1 (1.1%) unspecified.

The clinical and dermoscopic margins of the tumor lesions coincided in 29 lesions (33%), while were different in 59 lesions (67%).

Of the 59 lesions in which the clinical and dermoscopic margins did not coincide, 10 (16.9%) presented, in the lesion area identified by the dermoscope, classical criteria for BCC and 57 (96.6%) non-classical criteria. Classical and/or non-classical criteria were present in all lesions.

Classic criteria included: arborizing vessels (3 cases out of 59, 5.1%), ulcerations (2 cases out of 59, 3.4%), leaf-like areas (4 cases out of 59, 6.8%) and blue-gray globules (1 case out of 59, 1.7%). No lesions presented ovoid nests and spoke-wheel areas. Among the lesions with dermoscopic margins different from clinical margins, 49 (47 BCCs, 1 keratoacanthoma and 1 junctional nevus) did not present classical dermoscopic criteria.

Among the non-classical criteria of BCC, the most frequent were short telangiectasias (40 cases out of 59, 67.8%) and pink white areas (44 cases out of 59, 74.6%), found associated in 29 cases. Less frequent were in focus dots (4 cases out of 59, 6.8%), polarized structures (rosette/white streaks) (2 cases out of 59, 3.4%) and small erosions (1 case out of 59, 1.7%). No lesions showed concentric structures, blue-whitish veil and milia-like cysts.

Sensitivity, specificity, positive and negative predictive values and accuracy with the different dermoscopic criteria (classical, non-classical, combined) are shown in Table 3.1.

Statistical analysis showed that 8 BCCs (13.6%) presented both classical and non-classical criteria; 2 BCCs (3.4%) presented only classical criteria, while 49 lesions (83.1%) presented non-classical criteria (but not classical ones).

Lesions with dermoscopic margins different from clinical margins and lesions where dermoscopic and clinical margins coincided did not differ for maximum diameter (9.3±5.6 mm vs 9.9±6.9, p = ns).

Table 3.1. Sensitivity, specificity, positive and negative predictive values and accuracy with the different dermoscopic criteria (classical, non-classical, combined)

Classical criteria	**BCC**	**Non-BCC**	Sensitivity	0.175 (95% CI: 0.077-0.274)
present	10	0	Specificity	1 (95% CI: 1-1)
not present	47	2	Positive predictive value	1 (95% CI: 1-1)
			Negative predictive value	0.041 (95% CI: -0.015-0.096)
			Precision	0.203
Classical criteria	**BCC**	**Non-BCC**	Sensitivity	0.965 (95% CI: 0.917-1.013)
present	55	2	Specificity	0 (95% CI: 0-0)
not present	2	0	Positive predictive value	0.965 (95% CI: 0.917-1.013)
			Negative predictive value	0 (95% CI: 0-0)
			Precision	0.932
Combined criteria	**BCC**	**Non-BCC**	Sensitivity	1 (95% CI: 1-1)
present	57	2	Specificity	0 (95% CI: 0-0)
not present	0	0	Positive predictive value	0.966 (95% CI: 0.92-1.012)
			Negative predictive value	---
			Precision	0.966

CI = confidence interval

In relation to the histotype, calculations were made only on the two most frequent variants, nodular and superficial, as the other varieties were numerically too small for statistical analysis. Of 51 nodular BCCs, 28 (54.9%) had modified margins on dermatoscopic examination and 23 (45.1%) did not (p=0.62). The difference was instead significant for the 27 superficial BCCs, where the figures were 23 (85.2%) and 4 (14.8%), respectively (p=0.006).

In relation to the site of the lesions, no significant differences were found (p=0.85) between the number of lesions with and without modifications of the margins on dermatoscopic examination (Table 3.2).

Table 3.2. Frequency of differences between clinical and dermoscopic margins in various body areas

	Difference between clinical and dermoscopic margins	
Body area	Yes	No
Head-neck	18	9
Upper limbs	7	5
Lower limbs	3	0
Chest	28	14
Abdomen	3	1

DISCUSSION

Basal cell carcinoma is the most common form of skin cancer, with an incidence that has increased over the last decades.[13] Management of BCC can include surgical or nonsurgical approaches and depends upon lesion characteristics (location, type) and patient-specific factors (age, comorbidities, immunosuppression), as well as availability and costs of treatment options. Traditionally, standard excision is the treatment of choice.[6] More advanced and precise surgical approaches, such as MMS, are time-consuming, expensive and not easily available in many places around the world.[8]

In case of incompletely excised lesions, the probability of local recurrence ranges from 30% to 50%.[14]

Before surgery, an adequate determination of tumor margins is then crucial, in order to achieve radical removal. In this regard, several noninvasive methods have been proposed to improve precision, and, among these,

dermoscopy is likely to be the fastest and least expensive technique, other than essentially free of complications.[11,15,16]

Our data confirm the additional value of dermoscopy in the presurgical assessment of tumoral margins, compared with clinical examination alone, expecially in non-pigmented or partially pigmented lesions.[17,18, 19] Indeed, in our population, surgery based on margins assessed with naked eye would have led to an incomplete tumor excision in 2/3 of cases.

With regard to the histological type, the modification of the margins on dermoscopic examination is mainly present in superficial BCCs (85.2%), unlike nodular ones, which more rarely present this modification.

The usefulness of dermoscopy for a better definition of the margins of BCCs, with substantial improvement of the performance of surgical excision, has been reported in literature.[11,19] In 2010, Caresana and Giardini have introduced the concept of *apophatic* pattern, to describe the dermoscopic features of the peripheral areas of dermoscopy-detected BCCs, characterized by the interruption of the normal skin texture.[20] However, to the best of our knowledge, the dermoscopic features of the area between clinically and dermoscopically defined margins have not been studied.

In this area, we observed classical dermoscopic features of BCC, such as arborizing vessels (5.1%), ulcerations (3.4%), leaf-like areas (6.8%) and blue-gray globules (1.7%), but also, notably, non-classical features,

including pink-white areas (74.6%), short telangiectasias (67.8%), in focus dots (6.8%), polarized structures (rosette/white streaks) (3.4%) and small erosions (1.7%). In literature, pink-white areas and short telangiectasias have been reported to occur most frequently in superficial BCCs. This fits well with our observation of a higher occurrence of differences between clinical and dermoscopic margins in this histotype.

Classical dermoscopic criteria which represent the mainstay of the diagnosis of BCCs appear less useful in the definition of the margins of the tumor: based on our analysis, they allow a correct decision only in 20.3% of cases. A significantly better performance is achieved when considering non-classical dermoscopic criteria, whose presence correctly identifies margins in 93.2% of cases. Combined use of classical and non-classical criteria further improves the accuracy to 96.6%.

Our data also show that the frequency of these criteria is similar in BCCs located in different body areas, suggesting that they are tumor-specific and independent from the characteristics of skin in various districts.

CONCLUSION

Our study confirms and strengthens the value of dermoscopy in the management of BCCs, not only from a diagnostic point of view, but also as

noninvasive tool to provide guidance in the delicate preoperative phase of margin definition.

The observation of the area between clinically and dermoscopically detected margins gives additional information useful for a better definition of the actual tumoral margins and, consequently, for a really radical excision.

The diagnostic dermoscopic criteria in this area seem to be at least in part different from those used for the identification of the central tumor tissue. However, further studies with larger, population-based sample are needed to confirm this finding.

REFERENCES

1. Lallas A, Argenziano G, Zendri E et al. Update on non-melanoma skin cancer and the value of dermoscopy in its diagnosis and treatment monitoring. Expert Rev Anticancer Ther. 2013; 13: 541-58.
2. Ghita MA, Caruntu C, Rosca AE et al. Reflectance confocal microscopy and dermoscopy for in vivo, non-invasive skin imaging of superficial basal cell carcinoma. Oncol Lett. 2016; 11: 3019-24.
3. Reiter O, Mimouni I, Gdalevich M et al. The diagnostic accuracy of dermoscopy for basal cell carcinoma: A systematic review and meta-analysis. J Am Acad Dermatol. 2019; 80:1380-8.
4. Yélamos O, Braun RP, Liopyris K et al. Usefulness of dermoscopy to improve the clinical and histopathologic diagnosis of skin cancers. J Am Acad Dermatol. 2019; 80: 365- 77.
5. Luz FB, Ferron C, Cardoso GP. Surgical treatment of basal cell carcinoma: an algorithm based on the literature. An Bras Dermatol. 2015; 90: 377-83.
6. Peris K, Fargnoli MC, Garbe C et al. Diagnosis and treatment of basal cell carcinoma: European consensus-based interdisciplinary guidelines. Eur J Cancer. 2019; 118:10-34.

7. Cumberland L, Dana A, Liegeois N. Mohs micrographic surgery for the management of nonmelanoma skin cancers. Facial Plast Surg Clin North Am. 2009; 17: 325-35.
8. Shriner DL, McCoy DK, Goldberg DJ, Wagner RF Jr. Mohs micrographic surgery. J Am Acad Dermatol. 1998; 39: 79-97.
9. Farhi D, Dupin N, Palangié A, Carlotti A, Avril MF. Incomplete excision of basal cell carcinoma: rate and associated factors among 362 consecutive cases. Dermatol Surg. 2007; 33: 1207-14.
10. Bogdanov-Berezovsky A, Cohen AD, Glesinger R, Cagnano E, Krieger Y, Rosenberg L. Risk factors for incomplete excision of basal cell carcinomas. Acta Derm Venereol. 2004; 84: 44-7.
11. Carducci M, Bozzetti M, Foscolo AM, Betti R. Margin detection using digital dermatoscopy improves the performance of traditional surgical excision of basal cell carcinomas of the head and neck. Dermatol Surg. 2011; 37: 280-5.
12. Terushkin V, Wang SQ. Mohs surgery for basal cell carcinoma assisted by dermoscopy: report of two cases. Dermatol Surg. 2009; 35: 2031-5.
13. Conforti C, Corneli P, Harwood C, Zalaudek I. Evolving Role of Systemic Therapies in Non-melanoma Skin Cancer. Clin Oncol (R Coll Radiol). 2019; 31: 759-68.

14. Venturini M, Gualdi G, Zanca A, Lorenzi L, Pellacani G, Calzavara-Pinton PG. A new approach for presurgical margin assessment by reflectance confocal microscopy of basal cell carcinoma. Br J Dermatol. 2016; 174: 380-5.

15. Conforti C, Giuffrida R, Vezzoni R, Resende FSS, di Meo N, Zalaudek I. Dermoscopy and the experienced clinicians. Int J Dermatol. 2019 Jun 20.

16. Conforti C, Giuffrida R, Retrosi C, Di Meo N, Zalaudek I. Two controversies confronting dermoscopy or dermatoscopy: nomenclature and results. Clinics in Dermatology. 2019; 37: 597-9.

17. Lallas A, Apalla Z, Argenziano G, Longo C, Moscarella E, Specchio F, Raucci M, Zalaudek I. The dermatoscopic universe of basal cell carcinoma. Dermatol Pract Concept. 2014; 4: 11-24.

18. Gualdi G, Monari P, Apalla Z, Lallas A. Surgical treatment of basal cell carcinoma and squamous cell carcinoma. G Ital Dermatol Venereol. 2015; 150: 435-47.

19. Giuffrida R, Conforti C, Di Meo N, Deinlein T, Guida S, Zalaudek I. Use of noninvasive imaging in the management of skin cancer. Curr Opin Oncol. 2019. [Epub ahead of print].

20. Caresana G, Giardini R. Dermoscopy-guided surgery in basal cell carcinoma. J Eur Acad Dermatol Venereol. 2010; 24: 1395-9.

CHAPTER 4

Correlation between electrical impedance spectroscopy and the clinical and dermoscopic grading of actinic keratoses

(Berger M, Giuffrida R, Zalaudek I, Eber E, Hofmann-Wellenhof R. Unpublished data)

BACKGROUND

Actinic keratoses (AKs) are prevalent in a high percentage of the elderly population and their incidence continues to rise. Due to the risk of developing into invasive squamous cell carcinoma (SCC) – especially in individuals with multiple AKs on a photodamaged skin (field cancerization) – patients at high risk should definitely be treated.[1]

AKs appear clinically as erythematous, skin-coloured or partly brown pigmented scaly and rough maculae, papules or hyperkeratotic plaques with a diameter of approximately 0.1 to 2.5 cm and are often better palpable than visible.[1,2]

The dermoscopic examination has become an essential noninvasive method for the diagnosis of AKs. It increases sensitivity compared to a merely clinical examination by visualizing vascular structures and pigment patterns invisible to the naked eye.[3,4]

Four criteria for the identification of AKs have been established, including erythema with a red pseudo-network around the hair follicles, whitish-yellow scaling, fine linear waved vessels around the hair follicles and

enlarged whitish-yellow hair follicles filled with keratotic material. The diagnostic sensitivity and specificity of the dermoscopy in the classical non-pigmented AK are according to data up to 98 % and 95 %, respectively[5]; for pigmented AKs diagnostic accuracy is considerably lower than in the classical AK.[4] Corresponding to the clinical grading of AKs, they are also subdivided into three dermoscopic morphological severities[2], as can be discerned from Table 4.1.

Table 4.1. Clinical and dermoscopic grading of actinic keratoses[2,6,7]

	Clinical Grading	**Dermoscopic Grading**
AK Grade 1	not very palpable (better palpable than visible)	Erythema with red pseudo network and discreet white scaling
AK Grade 2	well visible and palpable	Keratotic, whitish-yellow, enlarged hair follicles on an erythematous background ("strawberry pattern")
AK Grade 3	highly visible and hyperkeratotic	Extended hair follicles filled with horn material on a whitish-yellow, scaly background or whitish-yellow structureless areas

Nevisense® (SciBase AB, Stockholm, Sweden) is a noninvasive diagnostic tool based on electrical impedance spectroscopy (EIS) developed primarily for melanoma detection. EIS is approved for clinical use to aid in the diagnosis of melanocytic skin tumors and in distinguishing between benign and malignant lesions. It is based on the emission of electrical currents at various frequencies and the subsequent measurement of the electrical tissue

resistance. Nevisense® measures bio-impedance of the skin at 35 different frequencies, logarithmically distributed from 1.0kHz to 2.5MHz, at four different depths utilizing 10 permutations.[8,9] EIS is sensitive to abnormal changes - predominant in malignant lesions - in cell structure, cell size and shape, cell membrane, intra- and extracellular environment.[10]

The diagnostic algorithm of EIS was developed based on previous studies, in which EIS score values from 1 to 3 are to be evaluated as EIS negative (benign) and from values of 4 to 10 as EIS positive (malignant).[8]

OBJECTIVES

The aim of this study was to correlate the EIS results with clinical and dermoscopic grading as well as to evaluate the diagnostic accuracy of EIS in the diagnosis of AKs and subclinical lesions in comparison to the naked eye examination and dermoscopy. A third objective was the investigation of a possible improvement of the EIS Score after topical field therapy of the AKs.

METHODS

This monocentric, prospective, non-randomized study was conducted at the University Clinic for Dermatology Graz during the period from November 10, 2017 to June 30, 2018. The study was approved by the Regional Ethical Review Board (29-476 ex 16/17).

Patients aged between 18 and 100 years with at least three AKs (and therefore suspected field cancerization) in the face, on the non-hairy scalp or on the back of the hands with Fitzpatrick type 1, 2 or 3 were considered eligible to enter the study. Patients not meeting EIS measurement criteria (see below), having had topical or other type of field treatment on the face, scalp or back of the hand two months before study inclusion, having insufficient patient notes or with clinical or dermoscopic images of poor quality were excluded.

EIS specific measurement/exclusion criteria:[8,9]

- Lesion with a diameter of less than 2 mm and greater than 20 mm
- Lesions on hairy skin
- Skin areas with other skin diseases (e.g. eczema, psoriasis, etc.) or scars
- Lesions on the trunk or extremities (except for the back of the hands).

First, in each patient a Test-AK was selected by a dermatologist, evaluated regarding clinical and dermoscopic features and classified into Grade 1-3. Then, a clinical and a dermoscopic image were taken using a digital MoleMax™ system by Derma Medical Systems.

Subsequently, the EIS measurements were carried out by one of two certified users (MB, GR) with the Nevisense® device, which is equipped with a probe and a disposable electrode of 5×5 mm.[8,9] The AK, a clinically unremarkable skin area in the vicinity of the lesion (suspected subclinical lesion) and a negative control on not sun-exposed skin behind the ear were examined with EIS and the resulting EIS scores were stored in the device as well as in Case Report Form. Four weeks after completion of topical treatment in ten out of 50 patients a follow-up appointment took place (Figures 4.1 and 4.2).

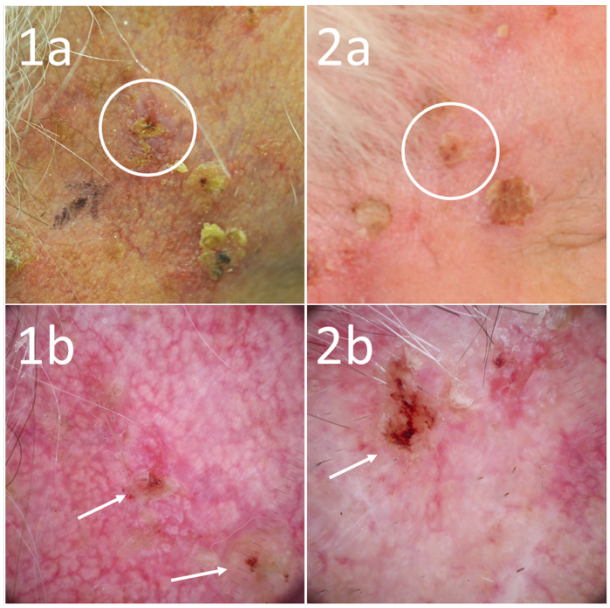

Figure 4.1. Actinic keratosis at baseline visit (1a, 1b) and follow-up (2a, 2b). The EIS Score was 8 at baseline as well as at the follow-up visit four weeks after termination of topical therapy with Zyclara®. The lesion was evaluated clinically as grade 3 with distinct hyperkeratosis (circled areas in 1a and 2a) at both visits. Dermoscopically the lesion appeared with "strawberry pattern", whitish-yellow structureless areas (1b, 2b) as well as ulceration (arrows in 1b and 2b) and was evaluated as grade 3 at both baseline and follow-up visit.

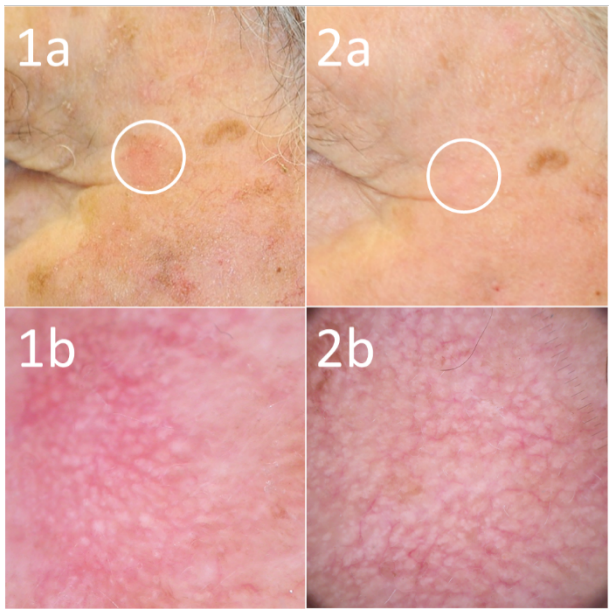

Figure 4.2. Actinic keratosis at baseline (1a, 1b) and follow-up visit (2a, 2b). The EIS Score was 7 at baseline and 3 at the follow-up four weeks after topical therapy with Picato® gel. The lesion was evaluated clinically as grade 3 with visible erythema (circled area in 1a), but it had clinically improved to grade 1 at the follow-up visit with no further erythema visible (circled area in 2a). Dermoscopically the lesion showed a "strawberry pattern" (1b, 2b) and was evaluated as grade 2 at baseline as well as at follow-up.

The results of EIS were compared with clinical and dermoscopic diagnostics to calculate Spearman's correlation coefficient as well as sensitivity and specificity with respect to clinical diagnosis used as the gold standard, since no further excision and histopathological analysis were performed. Despite the small sample size of ten patients, the follow-up EIS results of the AKs were also compared with those of the initial examination in order to detect a possible decrease in the EIS values if the therapy had been successful. Statistical analysis was carried out with the IBM SPSS Statistics 23 program.

RESULTS

Of 55 patients, which were initially included in the study and examined clinically, dermoscopically and with EIS during the study period (Table 4.2), a total of 50 patients (13 women and 37 men) with 50 Test-AKs were eligible for analysis (Table 4.3). The median age of the patients was 78 years (range 58 to 91 years).

Table 4.2. Reasons for exclusion of lesions from the statistical analysis.

Reason for exclusion	**Number of lesions**
Included lesions	55
- Withdrawal	2
- Inability to obtain a reference measurement	2
- Device failure	1
Eligible lesions	50

Table 4.3. Demographic data of the patients and clinical/dermoscopic characteristics of eligible AKs

Lesion	Sex	Age	Location	Therapy	EIS Score – AK	Clinical Grade – AK	Dermoscopic Grade – AK	EIS Score – PLS	EIS Score – NSES	Follow-up EIS Score – AK	Follow-up Clinical Grade – AK	Follow-up Dermoscopic Grade – AK	Follow-up EIS Score – PLS	Follow-up EIS Score – NSES	EIS Score difference – AK	Clinical grade difference – AK	Dermoscopic grade difference – AK	EIS Score difference – PLS
1	F	83	Head (scalp parietal left)		7	1	1	5	4									
2	M	60	Head (scalp parietal right)		6	1	1	6	4									
3	F	81	Head (right cheek)	Aldara®	7	3	2	2	3	5	2	2	4	2	-2	-1	0	+2
4	M	82	Head (scalp)	Zyclara®	6	1	1	7	4	4	1	1	6	3	-2	0	0	-1
5	F	83	Head (right pre-auricular region)		6	1	1	5	10									
6	M	84	Head (right frontal region)		9	2	2	7	5									
7	M	67	Head (right preauricular region)		5	1	1	4	3									
8	M	68	Head (left parietal region)		6	2	2	5	6									
9	M	72	Head (right temporal region)	Zyclara®	8	3	3	5	2	8	3	3	7	2	0	0	-1	+2
10	M	73	Head (left parietal region)	Picato® gel	7	2	2	5	8	3	1	2	5	2	-4	-1	0	0
11	M	79	Head (left parietal region)		6	2	2	3	6									
12	M	58	Head (right cheek)	Picato® gel	4	2	2	4	5	7	1	1	6	6	+3	-1	-1	+2
13	F	75	Head (left preauricular region)	Picato® gel	5	1	1	4	2	1	1	1	7	2	-4	0	0	+3
14	F	78	Head (right cheek)	Picato® gel	5	2	3	5	2	4	2	2	3	2	-1	0	-1	-2
15	M	62	Head (scalp)		3	3	3	4	1									
16	M	82	Head (left temporal region)		8	3	3	8	4									
17	M	84	Head (left cheek)		8	2	2	8	3									
18	M	64	Head (left cheek)		6	1	2	7	6									
29	M	74	Head (right cheek)		10	3	2	8	3									
20	F	74	Head (right cheek)		5	2	2	7	5									
21	M	84	Head (right cheek)		6	3	3	8	7									
22	F	79	Head (left cheek)		5	2	2	7	3									
23	F	90	Head (right nose)	Picato® gel	4	1	1	2	5	8	1	2	9	10	+4	0	+1	+7
24	M	91	Head (scalp)		5	2	2	3	4									
25	M	86	Head (right frontal region)	Picato® gel	10	3	3	9	5	9	3	3	8	5	-1	0	0	-1
26	M	88	Head (scalp)		9	3	3	9	9									
27	M	79	Head (right preauricular region)		10	3	3	9	7									
28	F	76	Head (right cheek)		10	3	3	8	10									
29	M	79	Head (frontal region)		9	2	2	9	2									
30	M	61	Head (scalp)		10	2	2	9	9									

Table 4.3 (continued)

Lesion	Sex	Age	Location	Therapy	EIS Score – AK	Clinical Grade – AK	Dermoscopic Grade – AK	EIS Score – PLS	EIS Score – NSES	Follow-up EIS Score – AK	Follow-up Clinical Grade – AK	Follow-up Dermoscopic Grade – AK	Follow-up EIS Score – PLS	Follow-up EIS Score – NSES	EIS Score difference – AK	Clinical grade difference – AK	Dermoscopic grade difference – AK	EIS Score difference – PLS
31	M	81	Head (right frontal region)	Picato® gel	8	2	2	7	6	8	2	2	7	8	0	0	0	0
32	M	78	Head (right frontal region)		9	2	2	8	5									
33	M	69	Hand (right back)		5	2	2	5	1									
34	M	82	Hand (left back)		7	3	3	6	4									
35	M	73	Head (left frontal region)		9	2	2	9	10									
36	F	77	Hand (right back)		10	3	2	3	1									
37	M	84	Hand (left back)		10	3	3	5	2									
38	M	87	Head (left frontal region)		10	3	3	9	10									
39	F	75	Head (left cheek)		10	2	2	6	4									
40	M	67	Head (right ear)		9	3	3	9	3									
41	M	77	Head (left cheek)		7	3	2	4	4									
42	M	77	Head (left frontal region)		5	2	2	3	1									
43	F	89	Hand (left back)		7	3	3	5	5									
44	M	74	Head (scalp)		4	1	1	3	5									
45	M	69	Hand (right back)		9	2	2	3	2									
46	M	81	Head (scalp)		9	2	2	4	1									
47	F	77	Head (right nose)		8	2	3	3	3									
48	M	85	Hand (right back)		8	1	1	9	4									
49	M	78	Head (right frontal region)		5	1	1	6	7									
50	M	79	Head (right frontal region)		10	1	1	10	2									

M=male; F=female; PLS= perilesional skin (suspected subclinical lesion); NSES=not sun-exposed skin (negative control)

The EIS score of the tested AKs correlated significantly with the clinical grading ($r=0.44$, $P<0.001$, $n=50$) and the dermoscopic grading ($r=0.31$, $P=0.031$, $n=50$) of the test AKs (Table 4.4).

Table 4.4. Correlation by Spearman between the Electrical Impedance Spectroscopy (EIS) scores and the gradings of the test AKs.

	EIS score AK*	n	p-value
Clinical Grading AK	0.438	50	**< 0.001**
Dermoscopic Grading AK	0.306	50	**0.031**

* Correlation coefficient

The Nevisense® score was compared with lesion severity and, as can be discerned in Figures 4.3 and 4.4, a clear trend towards higher EIS score results with increasing clinical and dermoscopic severity of skin changes is evident.

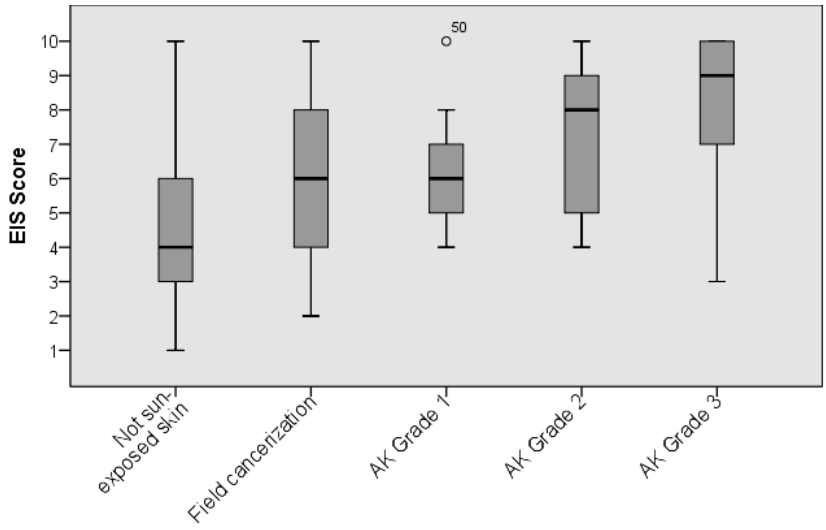

Figure 4.3. The clinical evaluation plotted against the EIS Score outcome. For each group, minimum value, first quartile, median, third quartile and maximum value are shown.

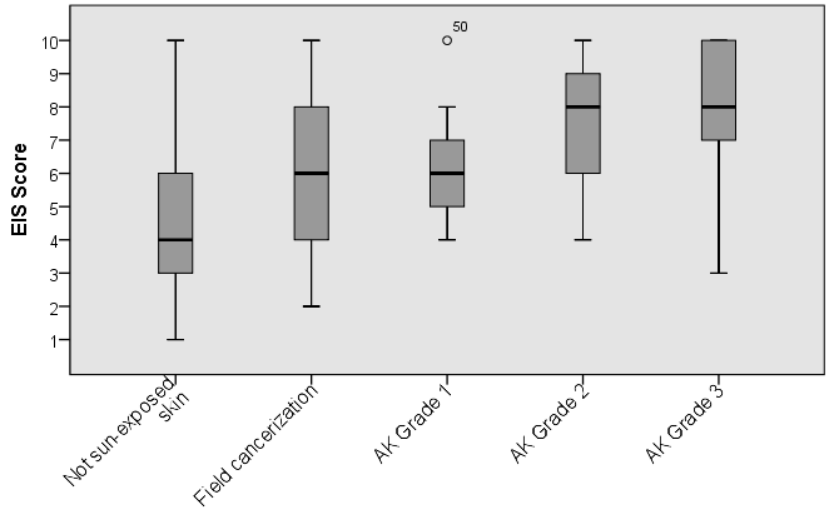

Figure 4.4. The dermoscopic evaluation plotted against the EIS Score outcome. For each group, minimum value, first quartile, median, third quartile and maximum value are shown.

Of the 50 lesions clinically and dermoscopically identified as AKs, 49 were detected as EIS positive, yielding a sensitivity of 98.0%.

In the immediate vicinity of the lesion without clinically and dermoscopically visible signs of AKs (suspected field cancerization), the measurements with EIS showed a positive result (EIS positive/malign) in 41 out of 50 cases (82.0 %).

From the negative controls in not sun-exposed skin areas the EIS measurements resulted in a negative result (EIS negative/benign) in 19 out of the 50 cases (38.0 %). Therefore, this method achieved a specificity of 38.0 %.

The EIS values of the AKs after field therapy were not significantly lower than at the first examination (Z=-0.846, P=0.397, n=10; Wilcoxon matched pairs rank test).

Out of the ten tested AKs at follow-up the Nevisense® measurements resulted in a lower EIS score in six lesions (60 %). Of these lesions, three showed clinical/dermoscopic improvement and three showed the same grade of severity. Importantly, the clinical and dermoscopic gradings were only lower in five out of ten evaluated lesions (50%).

There were no serious side effects or adverse events due to the use of the device during the entire study. Of 55 patients examined with EIS, one person (1.8%) reported pain during the EIS measurement and therefore withdrew the consent to participate in the study.

CONCLUSION

Due to the high prevalence rates of AKs in the elderly population, the frequent presence of multiple AKs with field cancerization[11] and the low risk of progression of individual AKs to invasive SCC [2,12], the diagnosis of AKs is largely based on the evaluation of clinical and dermoscopic criteria.

An additional tool in diagnostics and a decision-making aid regarding excision of the AK would be advantageous in everyday clinical practice.

While several studies have already investigated the safety, as well as the sensitivity and specificity of the EIS method, especially in the differentiation of melanomas and benign nevi, this is the first independent study, to our knowledge, on EIS with a focus on AKs.

In particular, the statistically significant correlation between the EIS results and the clinical grading (r=0.44) indicates a potentially clinically relevant relationship.

Therefore, the EIS could also be helpful in unclear cases as an additive method for determining the severity of AKs.

The observation that the EIS results correlated less with the dermoscopic grading (r=0,31) could be due to lack of experience in dermoscopy of AKs and their severity classification. Otherwise the dermoscopic criteria, according to which the severity of the AKs was determined in this study, could not necessarily be related to the changes of the cell structure recognized by the EIS.

Higher EIS values were achieved with increasing clinical and dermoscopic severity.

Interestingly, similarly high EIS scores were achieved for the suspected subclinical lesions as well as for the clinically and dermoscopically evaluated AKs grade 1. This reinforces the concept of field cancerization, which states that in a field of chronically sun-damaged skin malignant keratinocytes are present between the clinically visible lesions or in their surroundings.[3] These cells destroy the normal cell architecture – although not visible – and may therefore be detectable through Nevisense®. Moreover, the EIS results in the alleged subclinical lesions were positive for

malignancy in 82.0 %. Thus, we suggest that EIS could constitute a new noninvasive method to confirm a suspected field cancerization by a further diagnostic method and to indicate the need of field therapy.

No significantly lower EIS values could be achieved at a follow-up appointment, which can probably be explained by the small sample size of ten patients. The clinical and dermoscopic follow-up gradings of these patients were not lower in half of the cases. This could be explained by a lack of therapy response, low therapy effectiveness or – in the case of topical treatment – by a lack of compliance.

A drawback of the method is the low specificity of the applied algorithm. Table 4.3 shows that the EIS measurements on the negative controls yielded a positive result in 31 out of 50 (62.0 %) measurements and would therefore have detected malignancy in not sun-exposed and clinically “healthy” skin. This high rate of positive results may partly be attributed to the unfavorable choice of the negative controls behind the ear, as this body region may not always have been adequately protected from the sun and may therefore not meet the definition of "non-sun-exposed skin" in all cases. Another explanation could be the underlying tissue while performing EIS measurements, primarily the position of the probe on the skin directly above the bone (mastoid process), which could have led to erroneously high EIS values.

Furthermore, it raises the question of whether the algorithm, which was primarily developed for melanocytic lesions, should be modified for non-melanocytic lesions in further studies, for example defining a higher EIS Score cut-off predicting malignancy, to achieve a higher specificity of the method.

There are several limitations to this prospective study. It was monocentric and the sample size was relatively small. Furthermore, the clinical and dermoscopic diagnostics were used as the gold standard for diagnosis of the AKs, which were all not excised. A histopathological diagnosis and grading of the lesions would perhaps have allowed for a more certain evaluation but was not considered ethical to carry out in patients with multiple AKs, where field therapy represents the standard of care.

EIS measurements on AKs in this study showed similar sensitivity and specificity compared with previous studies on EIS. However, the studies are not directly comparable as they used mostly histopathological analysis as gold standard and specificity was based on lesions with clinical suspicion of malignancy, which were later on to be confirmed as histopathologically benign[8,9], instead of being based on clinically unremarkable skin. On the other hand, previous studies focused primarily on melanocytic lesions and involved only few AKs.

Based on the EIS score results gained in this study and other ongoing trials on NMSC the company that produces Nevisense® will develop an algorithm specifically for AKs/NMSC in conjunction with a new electrode for NMSC. Hopefully, this will contribute to a higher specificity of the method and entail further clinical benefit in NMSC detection.

Yielding a high sensitivity, EIS may be used by experienced dermatologists as an additional tool in diagnostics of AKs in everyday clinical practice, in particular to obtain further information about lesion severity. Additionally, it may reduce costs and patient morbidity in cases with no need to cut, when used in conjunction with the clinical evaluation of AKs.

REFERENCES

1. Strunk T, Szeimies R-M. [Actinic keratoses. Pathogenesis, clinical aspect and modern therapeutic options]. Hautarzt. 2014; 65: 241-4.
2. Zalaudek I, Piana S, Moscarella E et al. Morphologic grading and treatment of facial actinic keratosis. Clin Dermatol. 2014; 32: 80-7.
3. Malvehy J. A new vision of actinic keratosis beyond visible clinical lesions. J Eur Acad Dermatol Venereol. 2015; 29:3-8.
4. Zalaudek I, Argenziano G. Dermoscopy of actinic keratosis, intraepidermal carcinoma and squamous cell carcinoma. Curr Probl Dermatol. 2015; 46: 70-6.
5. Huerta-Brogeras M, Olmos O, Borbujo J et al. Validation of dermoscopy as a real-time noninvasive diagnostic imaging technique for actinic keratosis. Arch Dermatol. 2012; 148:1159.
6. Werner RN, Stockfleth E, Connolly SM et al. Evidence- and consensus-based (S3) guidelines for the treatment of actinic keratosis - International League of Dermatological Societies in cooperation with the European Dermatology Forum - Short version. J Eur Acad Dermatol Venereol. 2015; 29: 2069-79.
7. Costa C, Scalvenzi M, Ayala F, Fabbrocini G, Monfrecola G. How to treat actinic keratosis? An update. J Dermatol Case Rep. 2015; 9: 29-35.

8. Malvehy J, Hauschild A, Curiel-Lewandrowski C et al. Clinical performance of the Nevisense system in cutaneous melanoma detection: an international, multicentre, prospective and blinded clinical trial on efficacy and safety. Br J Dermatol. 2014; 171: 1099-107.
9. Mohr P, Birgersson U, Berking C et al. Electrical impedance spectroscopy as a potential adjunct diagnostic tool for cutaneous melanoma. Skin Res Technol. 2013;19: 75-83.
10. https://scibase.com/. Zugriff am 21. Mai 2018.
11. Eder J, Prillinger K, Korn A, Geroldinger A, Trautinger F. Prevalence of actinic keratosis among dermatology outpatients in Austria. Br J Dermatol. 2014; 171: 1415-21.
12. Werner RN, Sammain A, Erdmann R, Hartmann V, Stockfleth E, Nast A. The natural history of actinic keratosis: A systematic review. British Journal of Dermatology. 2013; 169: 502-18.

CONCLUSION

The vast and variegated world of noninvasive imaging used in Dermatology includes several techniques based on various physical principles and with different experimental stages of development. Some of them are already consolidated and used in routine clinical practice, others, even if well described in literature, are expensive and available only in few specialized centers. Finally, novel noninvasive imaging devices are currently under investigation, alone or in combinations thereof, and are expected to increase and facilitate the management of patients affected by skin cancers in the near future.

The data collected and analyzed during my PhD in Messina and Graz confirm the pivotal role of noninvasive imaging in both diagnostic and therapeutic phase of dermato-oncology and suggest possible additions and/or changes to currently employed criteria. In detail:

- we demonstrated and described for the first time the different clinical and dermoscopic features of melanomas associated with congenital or non-congenital nevi and their correlation with specific patients' characteristics, opening the way to a facilitation of the early recognition of melanoma;
- we reported the dermoscopic findings in the previously unexplored area between clinically and dermoscopically detected margins of basal

cell carcinomas, useful to achieve a radical excision of the tumor, with expected significant improvement of prognosis;

- we evaluated the possible usefulness of electrical impedance spectroscopy in the management of actinic keratoses, obtaining preliminary data which suggest good sensibility but low specificity, probably related to the use of a non-specific algorithm and consequently likely open to improvement in the future.

These already promising perspectives warrant further research in this field on a larger sample of patients with different ethnic and phenotypic characteristics.

“Somewhere, something incredible is waiting to be known” said once Carl Sagan, and, in the same spirit, we will continue our research trying to make the most of the advancements and innovations of imaging in dermato-oncology and having always as primary objective the patient’s health and satisfaction.